Han *et al. Energy Mater* 2023;3:300013
DOI: 10.20517/energymater.2022.77

Energy Materials

Review

Open Access

Check for updates

Progress in the high-temperature synthesis of atomically dispersed metal on carbon and understanding of their formation mechanism

Guokang Han[1], Wei Zhang[1], Lingfeng Li[1], Jiannan Du[1], Yuqi Yan[1], Lin Geng[2], Yujin Tong[3], Chunyu Du[1,*]

[1]School of Chemistry and Chemical Engineering, Harbin Institute of Technology, Harbin 150001, Heilongjiang, China.
[2]School of Materials Science and Engineering, Harbin Institute of Technology, Harbin 150001, Heilongjiang, China.
[3]Faculty of Physics, University of Duisburg-Essen, Duisburg 47057, Germany.

Correspondence to: Prof. Chunyu Du, School of Chemistry and Chemical Engineering, Harbin Institute of Technology, No. 92, Xidazhi Street, Nangang District, Harbin 150001, Heilongjiang, China. E-mail: cydu@hit.edu.cn

How to cite this article: Han G, Zhang W, Li L, Du J, Yan Y, Geng L, Tong Y, Du C. Progress in the high-temperature synthesis of atomically dispersed metal on carbon and understanding of their formation mechanism. *Energy Mater* 2023;3:300013. https://dx.doi.org/10.20517/energymater.2022.77

Received: 12 Nov 2022 **First Decision:** 19 Jan 2023 **Revised:** 3 Feb 2023 **Accepted:** 14 Feb 2023 **Published:** 3 Apr 2023

Academic Editor: Keyu Xie **Copy Editor:** Fangling Lan **Production Editor:** Fangling Lan

Abstract

The development of various high-performance electrochemical devices is crucial for mitigating the global climate crisis, and thus the design and fabrication of advanced electrode materials is highly significant. Currently, atomically dispersed metal on catalysts (ADMCs) have shown great potential in boosting the performance of various energy storage/conversion devices involving aqueous and aprotic catalytic processes, including fuel cells, water electrolyzers, CO_2 electrolyzers, metal-air batteries, and metal-sulfur batteries, as well as systems involving noncatalytic deposition/adsorption of metals. To date, several reliable fabrication methodologies that can ensure the formation of ADMCs have been demonstrated, and continuous optimization is still being performed. To further reinforce the basic scientific research and promote possible practical applications of these materials, we have analyzed, compared, and summarized progress in the fabrication methodology and formation mechanism of ADMCs in this review. This review aims to draw a comprehensive picture of the current methodology and underlying mechanism in the field of material fabrication to serve as guidance for future material design.

Keywords: Atomically dispersed metal, catalysis, energy conversion, carbon-based materials, formation mechanism

INTRODUCTION

The rapid development witnessed in the past several centuries has brought very severe global climate change, the consequent food crisis, social unrest, poverty, and human health challenges, that are affecting us all in one way or another[1,2]. Such an urgent situation has triggered rapidly increasing research worldwide on various electrochemical devices for energy conversion and storage, such as batteries, fuel cells, supercapacitors, and electrolyzers. It should be noted that the performance of these devices depends largely on the nature of the electrode materials, and therefore, designing and fabricating novel materials with the desired performance, low cost, durability, and easy manufacturability has been the center topic for the development of advanced electrochemical devices[3-8].

Atomically dispersed metals on catalysts (ADMCs) have been the focus of attention in the field of aqueous catalysis. The major advantage of ADMCs benefiting their utilization in catalytic systems is the combination of the intrinsic advantages of carbon materials, high electric conductivity, large surface area, and tunable porosity, with the maximized atomic utilization of metal centers. As a result, the specific activity of ADMCs with rational design can be remarkably greater than that of conventional metal catalysts. For example, when catalyzing the electrochemical oxygen reduction reaction (ORR), some atomically dispersed metals (ADMs) with various active metal centers, even nonprecious metals, are more active than benchmark Pt/C catalysts[9-12]. Similar phenomena can also be observed in hydrogen evolution reaction (HER)[13,14]. In addition, because metal centers in ADMCs are stabilized by surrounding nonmetallic atoms, it is possible to tune their electronic structure and adsorption properties by adjusting the coordination environment of metal atoms. As a result, the regulation of reaction selectivity on ADMCs can be achieved, benefiting their application in electrolyzers aimed at producing certain chemicals[15-18]. It was reported that the reaction pathway of oxygen reduction reaction can be tuned by adjusting the chemical nature of N in CoN_4 moieties. When coordinated by pyridinic N, Co atoms with high spin enable full reduction of O_2 to H_2O, and the reaction pathway can be altered to H_2O_2-selective in pyrrolic N bonded CoN_4[19].

Very recently, ADMCs have extended their effectiveness in various battery systems[20-22]. The possible application of ADMCs as the cathode material for Li-air batteries is based on the catalytic nature of the charge/discharge process in the cathode. For example, Ru ADMs are believed to be effective in accelerating sluggish ORR and oxygen evolution reaction (OER), decreasing the polarization of the Li-air battery[23]. Our group also found that Cu ADMs are able to regulate the morphology of Li_2O_2 during discharge and further accelerate its decomposition kinetics via a one-electron transfer mechanism during the subsequent charging process[24]. In addition, the performance of Li-S batteries can also be promoted by ADMCs. Besides, some ADMCs are capable of regulating the morphology of metal clusters during electroreduction and facilitating their uniform deposition, which is important to prevent dendrites and reinforce the safety of metal electrodes. As a result, ADMCs are showing potential application as anode materials in various metal-ion batteries, including traditional Li batteries and newly emerged Na-ion and Zn-ion batteries[25,26].

In addition to the remarkable performance enhancement brought in by ADMCs, the relatively uniform structure of ADMCs has provided a perfect platform for research on reaction pathways and detailed mechanisms[27].

Generally, isolated ADMs are extremely unstable due to the significantly increased surface free energy when downsizing bulk metals[28]. Thus, the successful fabrication of ADM-containing materials is the perfect example of precisely manipulating material chemistry to satisfy the needs of human beings. The present results strongly indicate that achieving a strong chemical interaction between ADMs and the support is critical for the successful fabrication of ADM-based materials[29]. This brief review focuses on research updates on the formation mechanisms of ADMCs. In addition, the fabrication methodologies, together with their correlation with the obtained coordination structure, are also reviewed and summarized. In the following sections, the correlation between the ADM structure and fabrication methods is first discussed, followed by a summary of the formation mechanism of ADMCs by high-temperature thermal-chemical reactions, trying to summarize the commonality among different procedures. The formation mechanisms are roughly subclassified into three types based on the reaction characteristics, including the transformation of pre-existing coordination structure, fixation via ligand replacement, and direct anchoring of metal atoms, as illustrated in Figure 1. The review ends with outlooks highlighting the future directions and challenges for scientific research on the fabrication methods of ADMCs and their formation mechanism.

GENERAL DISCUSSION

The formation process of functional materials has always attracted the interest of scientists. Behind the various chemical reactions that lead to the formation of the desired chemical composition or the required spatial structure are the reaction mechanisms. Uncovering the formation mechanism is important to provide useful methodologies for the development of suitable materials and valuable guidance for the further rational optimization of the process.

Commonalities and specialties of ADMCs

It has been found that ADMs can be stabilized in a wide range of substances through favored metal-metal or metal-nonmetal interactions between metal atoms and the support. For example, a small number of foreign ADMs can be stabilized within the metal bulk in the form of single-atom alloys [Figure 2A][30], and several metal oxides/hydroxides are capable of bonding foreign ADMs [Figure 2B-D] by oxygen species on the surface or coordination bonds into the lattice[31,32]. Similarly, there are reports on the utilization of metal heteropolymetalates/carbides as stabilizers [Figure 2E and F][33-37]. For carbon-based substrates, strong metal-substrate interactions via coordination bonds are also necessary.

However, unlike the abovementioned systems, the coordination structure of carbon-based ADMCs is more complicated. Judging from the local chemical environment, ADMCs can be roughly divided into two categories. The first one has metal centers coordinated by no more than two heteroatoms with a three-dimensional bonding geometry[38], as illustrated in Figure 2G. The second form of ADMCs, as reported by the majority of related work, has metal centers located at the vacancies of the carbon framework and coordinated by more than two nonmetal atoms from the carbon framework in a planar/quasi-planar position[39,40], as shown in Figure 2H.

Correlation between the ADMCs structure and the synthesis process

The formation of both forms of ADMCs is highly related to the nonmetal atoms as anchoring points, especially heteroatoms introduced into the carbon substrate. These dopants can be introduced by various doping agents either simultaneously with or before metal precursors, depending on the detailed fabrication process. To date, several methods have been proven to be effective in producing ADMCs. They can be roughly divided into three categories based on the reaction parameters critical for the formation of ADMs: thermal-chemical reactions, atomic layer deposition[41,42], and wet-chemical reactions[38,43]. Thermal reactions involve high-temperature treatment of a mixture of carbon sources, metal sources, and heteroatom doping agents, during which ADMs are formed. The reaction temperature varies from below 300 °C to above 1,000 °C, depending on the thermal behavior of the precursors and the targeted structure of ADMs in the product. In atomic layer deposition, metal-containing precursors are introduced into the reaction chamber, react in a controlled manner with the surface functional groups of the carbon substrate, and simultaneously fix the ADMs. Wet-chemical reactions usually involve metal ions in solution spontaneously adsorbed by N or other nonmetal elements from the carbon framework.

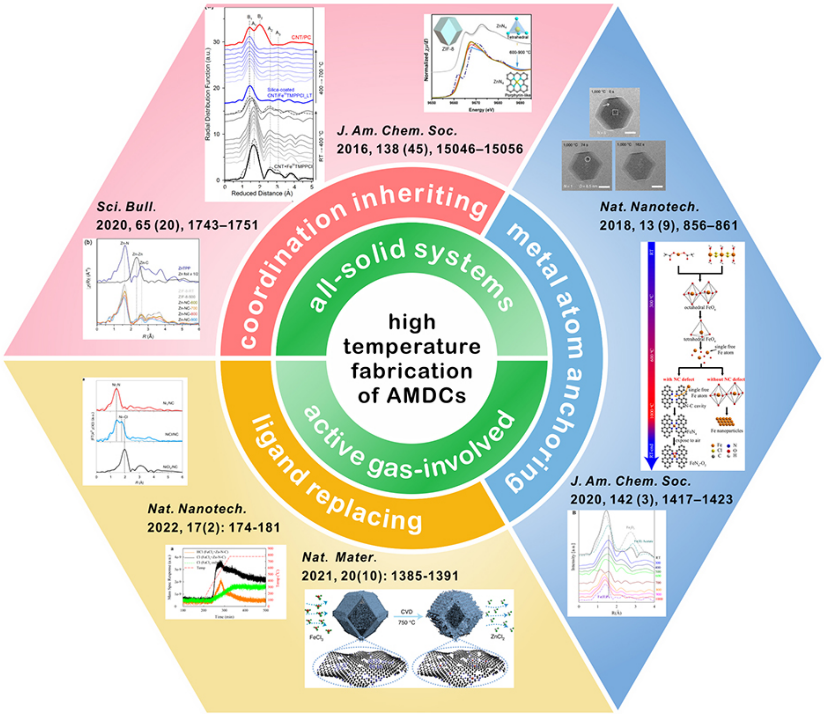

Figure 1. Illustration of the three formation mechanisms of ADMCs via thermal-chemical reactions

The embedded structure is generally constructed by simultaneously forming the central metal atoms and their surrounding coordination environment *in-situ* during a high-temperature reaction. Taking the most common MN_4 moieties as an example, there is evidence that during high-temperature pyrolysis processes, the formation of N_4 defects and their bonding with metal atoms occur at the same time[44-46], and the formation energy of MN_4 is smaller than that of N_4 defects on carbon frameworks[47]. A recent study has even shown that the vacancies that host metal atoms for carbon frameworks are unlikely to be formed in the absence of metal[48]. The formation of the second form of ADMs is usually related to wet-chemical reactions, and the following high-temperature treatment is avoided. In solution, metal ions can be spontaneously adsorbed by N or other nonmetal elements from the carbon framework, and the key to such a simple adsorption pattern is the separation of metal adsorption with substrate formation, i.e., the carbon framework as a substrate is already fully formed and does not undergo structural change during later metal adsorption[38]. Inferring from the current experimental evidence, the embedded form of ADMs is more energetically favored at high temperatures[49]. Thus, the transformation of the coordination environment can occur during the fabrication process when the metal ions adsorbed by heteroatoms convert into embedded ADMs.

It should be noted that the discussion here is only brief, and it is not sufficient to establish a certain correlation between the geometry of ADMCs and the synthesis process. In some cases, ADMCs with embedded MN_4 moieties can also be formed by wet-chemical reactions. For some, materials with isolated metal macrocyclic molecules adsorbed on carbon without heat treatment can sometimes be recognized as ADMCs as well, and the embedded nature of metal atoms in macrocyclic molecules remained after adsorption[50-52]. Another example is that metal atoms in solutions can be trapped by pre-existing N_4 structures from the carbon framework[39,43,53].

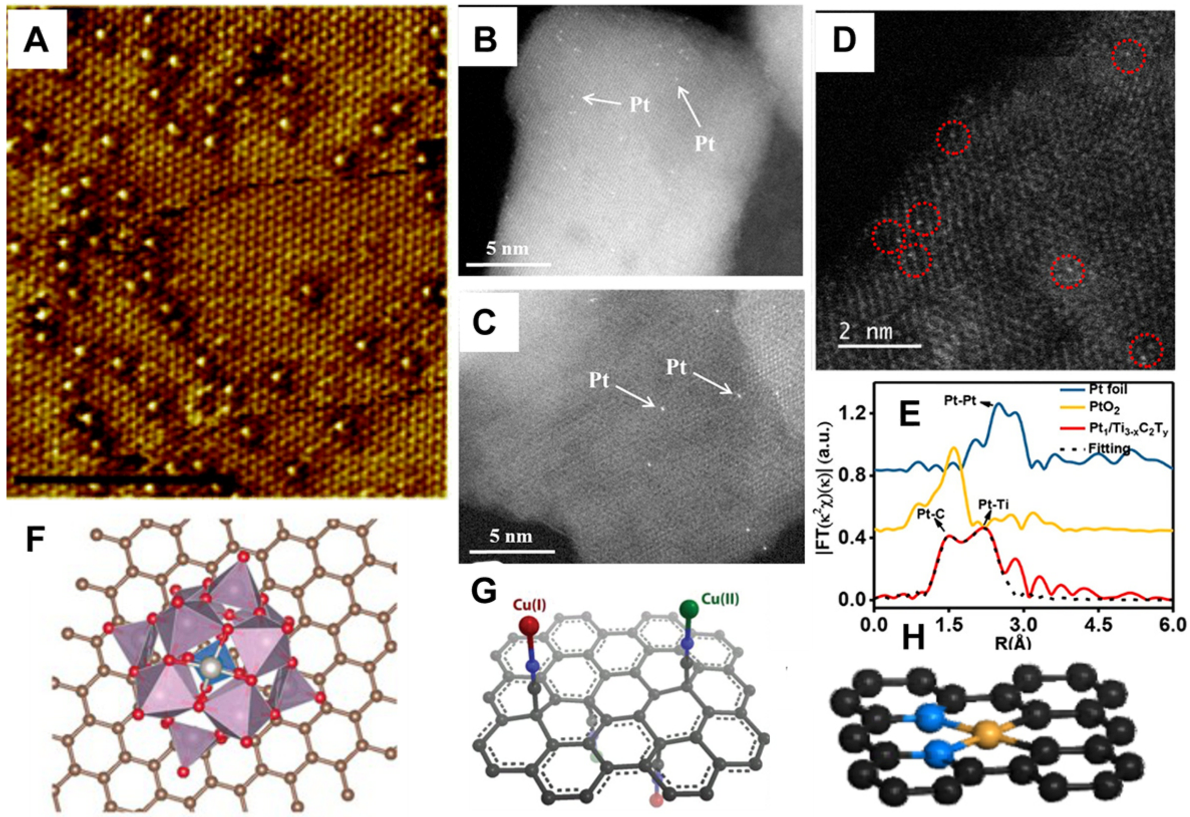

Figure 2. Characteristic results and illustration of ADMs on non-carbon substrates and illustration of ADMCs. (A) STM image of Pd/Cu single atom alloy with 0.01 ML Pd[30], reproduced from Ref.[30] with permission. Copyright 2013 Royal Society of Chemistry. (B and C) Aberration-corrected HAADF-STEM images of Pt_1/Fe_2O_3 and $Pt_1/\gamma\text{-}Al_2O_3$, respectively[31], reproduced from Ref.[31] with permission. Copyright 2017 American Chemical Society. (D) Aberration-corrected HAADF-STEM image of sAu/NiFe LDH[32], reproduced from Ref.[32] with permission. Copyright 2018 American Chemical Society. (E) Pt L3-edge EXAFS of $Pt_1/Ti_{3-x}C_2T_y$ and Ref.[33], reproduced from Ref.[33] with permission. Copyright 2019 American Chemical Society. (F) Illustration of the most stable configuration of Pt atom on phosphomolybdic acid/graphene[34], reproduced from Ref.[34] with permission. Copyright 2016 Wiley-VCH. (G and H) Illustration of Cu ADMCs formed by adsorption by surface -CN[38] and embedding into the carbon framework[40], reproduced from Ref.[38] (Copyright 2019 Wiley-VCH) and Ref.[40] (Copyright 2021 Springer Nature) with permission.

Techniques for studying formation mechanisms

To decode the formation process, knowing the change in substances during high-temperature treatment is necessary. The most common procedure to obtain such information is to perform temperature-dependent *ex-situ* characterization by stopping the thermal treatment at different temperatures and characterizing the as-prepared samples. By various phase, spectroscopic, and microscopic characterization techniques, the evolution of metal species can be reproduced, provided that no additional changes occur during the cooling process. A more accurate method is to perform *in-situ* characterization, during which the evolution of ADMs can be directly observed. Such techniques cannot be realized until recent years. The development of modern characterization techniques has granted us an unprecedented opportunity to look into the detailed structure of the materials of interest on the nanometer- and even sub-nanometer-scales. In the research of ADMCs, both spherical aberration-corrected transmission electron microscopy and X-ray absorption spectroscopy (XAS) have become irreplaceable in identifying ADMs as well as in revealing their detailed chemical composition and coordination structures. The high sensitivity of XAS to the local environment and the relatively fast data collection process make it possible to decode even the tiny temperature-dependent or time-dependent structural evolution of ADMs, opening the gate to unraveling the thermal-chemical reaction process.

Target of this review

The formation mechanism of ADMs seems direct and apparent in the early days when researchers began to treat ORR-active macrocyclic compounds with carbon support at high temperatures, hoping to stabilize these less stable compounds. It was expected that due to the similar chemical structure of the six-membered ring building block of carbon with macrocyclic compounds, the adsorption becomes stronger as the temperature rises. As proven by modern characterization techniques, ADMs can be fixed in situ into the conjugated carbon framework. However, the situation became more complicated when it was found that similar materials with ADMs can also be obtained by pyrolyzing a mixture of a proper carbon source with nitrogen- and metal-containing compounds. The production of ADMCs has been a "black box" for a long time, as we only know that ADMCs can be obtained by adding the right starting materials to the box and that the composition can be regulated by starting materials, temperatures, and pyrolysis processes, but the reaction mechanism remains unknown due to the complexity of the thermal reaction system and the interference of high temperatures.

This review focuses on high-temperature-based thermal reactions for fabricating ADMCs. One reason is that among all the methodologies, the high-temperature thermal-chemical reaction is the most widely adopted, especially for application in electrochemical devices, due to its enhanced electron conductivity by thermal treatment and relatively low cost (cheap precursors and needless high-end equipment). Another reason is that the formation mechanism of ADMCs through wet-chemical and ALD methods are much more straightforward to understand, and as a result, research on the formation mechanism through high-temperature-based thermal reactions, i.e., the changes during the transformation from metal precursors to ADMs, is at the center of scientific research. Such a mechanism is at the base of understanding the formation of ADMs, including hotspot materials with dual or multiple metal atoms, whose formation is even more complicated. In addition, it plays an important part in rationally choosing precursors as well as designing reaction routes to obtain targeting materials with desired coordination structures. However, to date, the understanding of the formation mechanism of ADMCs via thermal reactions remains quite primary. Considering that most ADMCs are developed mimicking macrocyclic compounds with MN_4 structures for electrochemical catalysis in the first place and have been mainstream catalysts until today, the following parts of this review will mainly discuss ADMCs fully or partially stabilized by N atoms, as they are the most commonly seen and studied.

Before moving into the detailed discussion on the fabrication mechanism of ADMCs, it is noteworthy that despite similar fabrication processes based on thermal reactions, the detailed emergence mechanisms of ADMs may vary from one system to another depending on the available observational evidence, suggesting that there is no universal pattern describing every scenario. However, on a relatively narrow scale, limited to the specific starting materials or reaction conditions, the similarities become clearer and can be summarized.

TRANSFORMATION VIA COORDINATION INHERITANCE

Evidence on the formation mechanism

The phrase "coordination inheritance" describes the situation where the major coordination environment of the metal atoms remains the same during the transformation from precursor to ADMs during thermal treatment.

The very first attempt to fabricate ADMCs was performed with macrocycle compounds. It is known that by pyrolyzing macrocycle compounds with carbon, the electrochemical stability of these molecules can be improved. Sa *et al.* studied the thermal evolution of Fe-based macrocycle compound, FeTMMPPCl, adsorbed on the surface of carbon nanotubes (CNTs) under a protective layer of SiO_2 using *in-situ* XAS[54]. As suggested by the in-temperature XANES shown in Figure 3A, the original 5-coordinated structure of FeTMMPPCl becomes a square planar FeN_4 configuration after the removal of axially-coordinated Cl at 400 °C, revealed by the disappearance of pre-edge feature A originating from the square pyramidal symmetry of FeTMPPCl, accompanied by the rising pre-edge feature B from a square planar D_{4h} symmetry. It is interesting to find that after SiO_2 coating, feature B disappears, suggesting the axial interaction between Fe and SiO_2, destroying the D_{4h} symmetry. The authors suggested that such an interaction is critical for resistance against aggregation. Combined with the EXAFS spectra shown in Figure 3B, it is clear that the FeN_4 structure can be maintained at a temperature as high as 700 °C before partially aggregating into Fe clusters at 800 °C, corresponding to the red lines labeled CNT/PC.

In addition to macrocyclic compounds, it is believed that there are MN_x species within the structure of ZIF-based precursors. Using temperature-dependent XAS, Wang *et al*. studied the coordination nature of Zn in ZIF-8 after being pyrolyzed at different temperatures ranging from 500 to 900 °C and acid washed to remove aggregated species[55]. The crystalline structure of ZIF-8 with tetrahedral ZnN_4 local coordination is not destroyed until 600 °C, as evidenced by the identical XANES and EXAFS spectra of ZIF-8 and ZIF-8-500 [Figure 3C and D]. When the temperature reaches 600 °C, the coordination configuration becomes planar similar to macrocyclic compounds with similar features in the XAS spectra. A weight ratio as high as 3 wt.% was detected for ZIF-8-600, suggesting that the stabilization of ZnN_4 moieties occurs at the very early stage of ZIF-8 carbonization. Although the research is only limited to ZIF-8, it is reasonable to believe that other metal ions coordinated by the imidazole ring in the ZIF framework can undergo similar processes and become ADMS after pyrolysis.

Applicable scenario

All-solid thermal-chemical reaction

The most applicable scenario for ADMCs' formation via coordination inheritance is the all-solid thermal-chemical reaction. It is the most traditional method for fabricating ADMCs, which can be dated back to when researchers tried to stabilize macrocyclic compounds by pyrolyzing these molecules with carbon[56]. Later, it was found that similar ADMs can be obtained by pyrolysis of simple metal salts with proper carbon and nitrogen precursors, opening the gate for the half-century-long exploration of ADMCs[57].

In all solid thermal-chemical reactions, all precursors are thoroughly mixed before undergoing simple pyrolysis in an inert or reducing atmosphere without intentionally introducing gaseous reactants from outside the system. The chemical changes can be rather complicated within the mixture at elevated temperatures, with multiple reactions occurring at the same time, including the formation of ADMs and further structure evolution[49], accompanied by[58,59]or independent from[60,61] heteroatom doping, depending on the nature of the chosen precursors. The pyrolysis parameters, pre- and post-pyrolysis treatments are also highly dependent on the type of precursors[62-64].

Organics as carbon precursors

The most commonly utilized carbon precursors are organics, which undergo carbonization during high-temperature pyrolysis, favoring the *in-situ* formation of ADMs. In general, metal-organic frameworks (MOFs), polymers, biomass, and simple organic molecules are the four types of most commonly seen carbon precursors for ADMCs.

In the past few years, metal-organic frameworks (MOFs) have been discovered as promising starting materials for ADMCs via high-temperature pyrolysis. To date, various MOFs, including Zn-based ZIF-8,

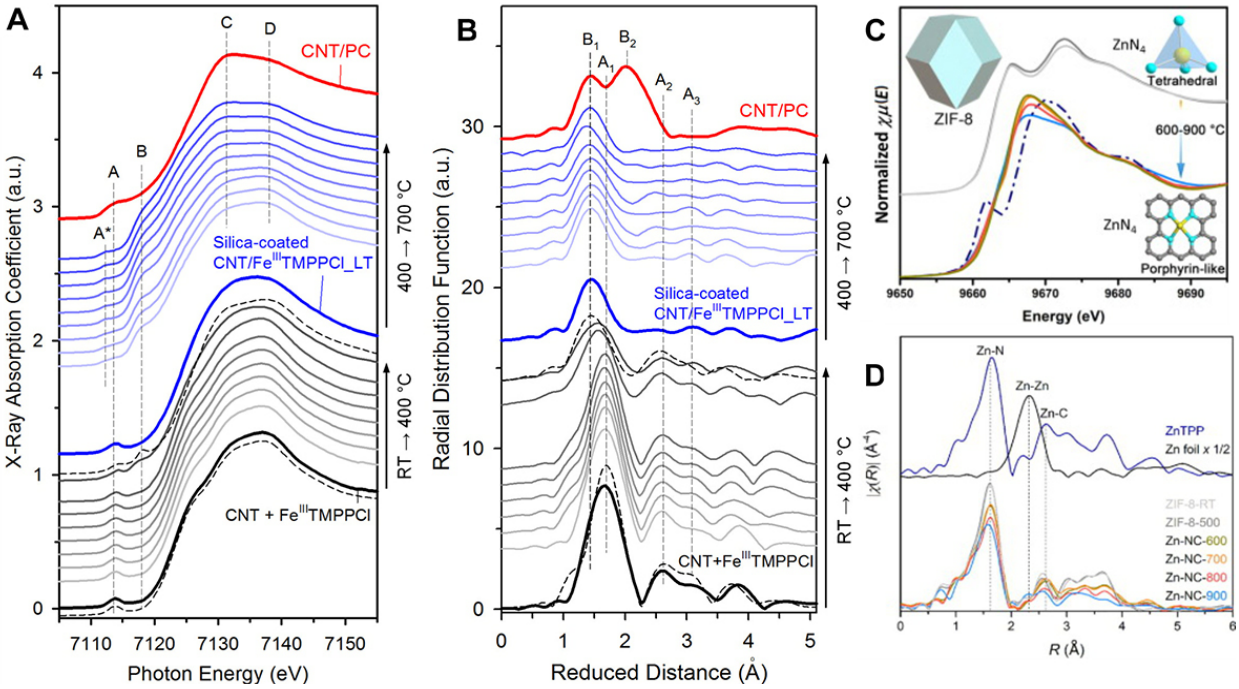

Figure 3. Thermal evolution of the metal center in macrocycle compound and ZIF-8 revealed by XAS. (A) In-Temperature Fe K-edge XANES, and (B) EXAFS spectra of FeTMPPCl[54], reproduced from Ref.[54] with permission. Copyright 2016 American Chemical Society. (C) Temperature-dependent Zn K-edge XANES, and (D) EXAFS spectra of ZIF-8 treated at different temperatures after acid wash[55], reproduced from Ref.[55] with permission. Copyright 2020 Elsevier.

Co-based ZIF-67[65], Zr-based MOF-545[66] and UiO-66[67], Al- and Ga-based MIL-53[68] and some other MOFs with Cd center[69], Mn center[70], Bi center[71] have been investigated as carbon precursor for ADMCs. The basic building blocks of MOFs consist of metal centers coordinated with organic linkers and are repeatedly arranged in three dimensions, forming an ordered pore structure, as illustrated by the example of ZIF in Figure 4A. Thus, most MOFs are extremely rich in micropores. The pore structure (porosity, pore size, and elemental composition) can be regulated by ligand molecular structure, providing an efficient way to construct the precursor composition and structure[72].

As mentioned above, ADMs on carbon are, in most cases, stabilized by heteroatoms within the carbon framework by forming coordination bonds. It is suggested that the existence of chemical bonds between metal atoms and the ligand through desired nonmetal atoms in the precursor is beneficial for the formation of ADMs. In some cases, metal-heteroatom coordination is so abundant and stable that no additional heteroatom source is needed to stabilize ADMs during carbonization. Such systems with fewer precursors make it easier for researchers to precisely control the chemical composition and structure of the precursor and to uncover the formation reaction mechanism. Zn-based zeolitic imidazolate framework-8 (ZIF-8) may be one of those MOFs with such advantages.

ZIF-8 is composed of Zn centers and N-containing 2-methylimidazole linkers. There are two critical features in ZIF-8 that are beneficial for the formation of ADMCs. One is the porosity of the resultant carbon. During the thermal carbonization process, as the organic linkers decompose while releasing gaseous products, the microporous structure can partially maintain within the carbon residuals[73], facilitating the formation of ADMs [Figure 4B and C]. Besides, the sublimation of metallic Zn generated from the reduction of Zn(II) by carbon during thermal treatment introduces even more micropores in the resultant.

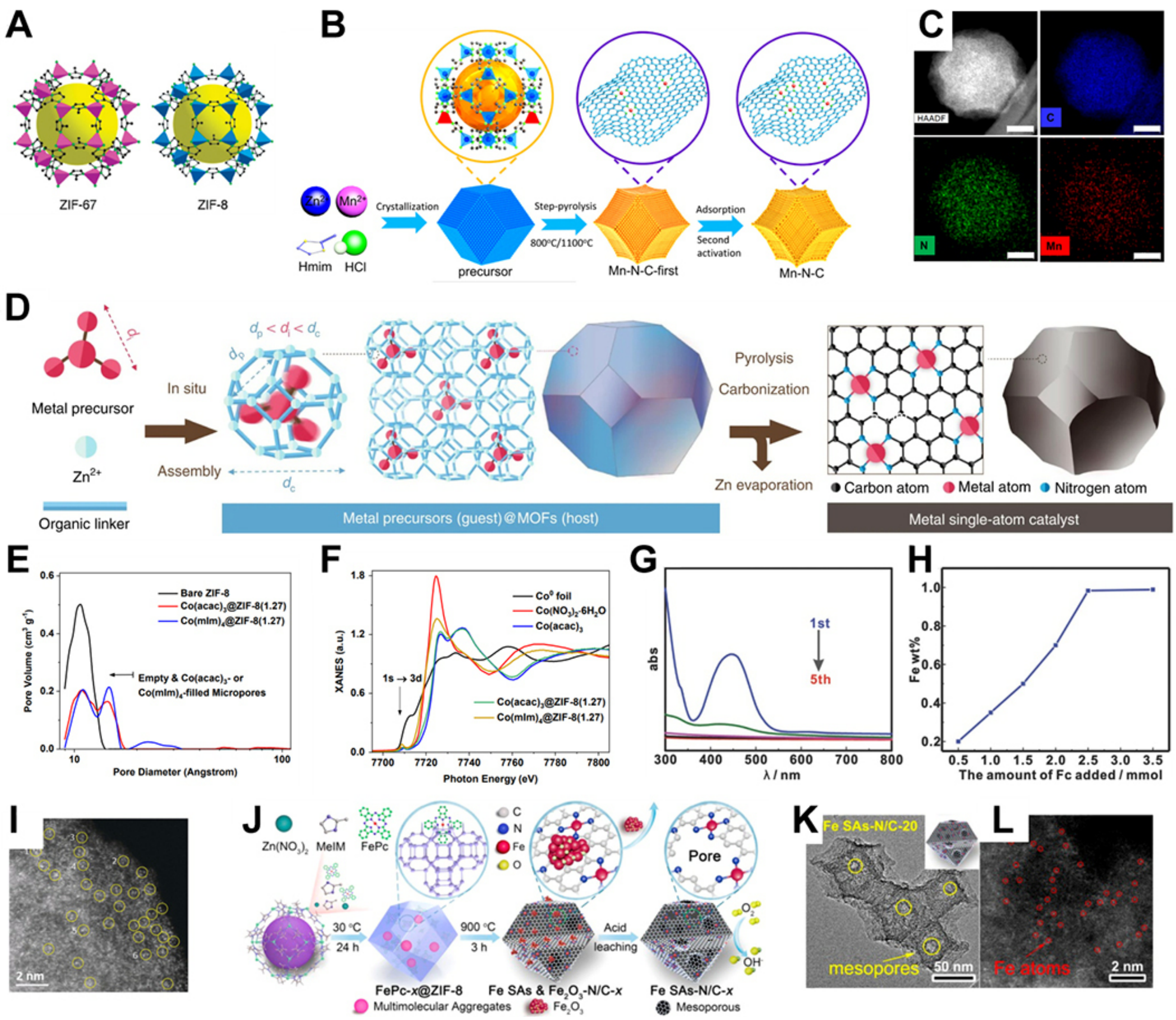

Figure 4. (A) Topological illustration of ZIF-67 and ZIF-8[72], reproduced from Ref.[72] with permission. Copyright 2010 American Chemical Society. (B) Illustration of the preparation of Mn-N-C via metal nods replacement and (C) HAADF-STEM image and EDS element mapping of Mn-N-C[73], reproduced from Ref.[73] with permission. Copyright 2020 American Chemical Society. (D) Illustration of the preparation of ADMCs via host-guest interaction[74], reproduced from Ref.[74] with permission. Copyright 2020 Springer Nature. (E) Pore diameter distribution of ZIF-8 and $Co(acac)_3$@ZIF-8 and (F) Co K-edge XANES spectra of $Co(acac)_3$@ZIF-8 and $Co(mIm)_4$@ZIF-8[75], reproduced from Ref.[75] with permission. Copyright 2020 Springer Nature. (G) UV-vis spectra of the centrifuged supernatant after different washing steps and (H) Fe weight ratio in different Fc@ZIF-8 *vs.* the amount of Fc added during the fabrication process[76], reproduced from Ref.[76] with permission. Copyright 2018 Wiley-VCH. (I) Aberration-corrected HAADF-STEM images of Ru_3@ZIF-8[77], reproduced from Ref.[77] with permission. Copyright 2019 Wiley-VCH. (J) Illustration of the preparation of defect-coupled FeN_4 via host-guest interaction and (K) TEM and (L) aberration-corrected HAADF-STEM images of Fe SAs-N/C-20[78], reproduced from Ref.[78] with permission. Copyright 2018 American Chemical Society.

Another important factor facilitating the usage of ZIF-8 as carbon precursors for ADMCs is element compatibility. Zn(II) centers in ZIF-8 can be replaced by Co(II) in all proportions and by many other transition metal cations for a small amount without compromising the crystal structure. The pre-existing metal-N bonding is considered vital for the stabilization of metal species in the form of ADMs [Figure 4B and C]. Besides direct chemical bonding, the special spatial structure of ZIF-8 with cavities as large as 11.6 Å and open pores of 3.4 Å is perfectly efficient in trapping single molecules within the cavities[74], shown in Figure 4D. Such host-guest interactions guarantee the mono-dispersion of these metal-containing molecules and are believed to be facilitative for the formation of ADMCs. Xie *et al.* suggested that after hybridizing $Co(acac)_3$ with ZIF-8 through host-guest interactions, the micropores at 9-13 Å substantially descend, and new pores at 13-17 Å arise [Figure 4E][75]. In addition, the XANES feature of $Co(acac)_3$@ZIF-8 differs much from $Co(mIm)_4$@ZIF-8, where Co ions are fixed as the metal nods in the framework of MOF [Figure 4F], providing evidence for the encapsulation of $Co(acac)_3$ into the cavities[75]. Additional evidence has been given by the research of Wang *et al*. The authors recorded the UV-vis signal of the supernatant from washing the Fc@ZIF-8 [Figure 4G] fabricated by adding ferrocene (Fc) during the regular methanolic synthesis of ZIF-8[76]. It was found that the ferrocene signal became absent in the supernatant after the fourth wash. The ICP-OES results suggested a Fe content of 1 wt.% left in the Fc@ZIF-8, indicating that the remaining Fc are stabilized by the ZIF-8 framework. Besides, it was shown in Figure 4H that adding up the amount of ferrocene as the starting material in the synthesis of ZIF-8 did not lead to a corresponding rise in the amount of ferrocene in the as-prepared Fc@ZIF-8, suggesting the saturation of ferrocene in ZIF-8. These results clearly suggest that Fc molecules are trapped within the cavities, in agreement with the molecular size of 6.4 Å for Fc and its correspondence to the pore structure of ZIF-8. Other guest molecules in successful demonstration including $Ir(acac)_3$[74], $Ru_3(CO)_{12}$[77] [Figure 4I], Fe-phthalocyanine[78] [Figure 4J-L], Fe-1,10 phenanthroline[79], $Rh(acac)_3$[80], $Fe(acac)_3$[81], $Ru(acac)_3$[64].

Although there are several ZIFs with compositions similar to that of ZIF-8, only ZIF-8 is the most utilized precursor for ADMCs. Wang *et al*. studied the thermal behavior of various Zn-based ZIFs with different imidazolate linkers[82]. It was found that due to various carbonization pathways, the chemical composition, surface properties, and graphitization level are highly related to the molecular structure of imidazolates. The 5-membered nature of the imidazole ring, in the absence of side chains, triggers carbonization coupled with denitrogenation, resulting in a higher graphitization level and leaving less N in the carbon framework. The methyl chain in 2-methylimidazole, however, is able to participate in the carbonization reaction, balancing the graphitization degree and N content, making ZIF-8 the most suitable precursor for ADMCs.

Thus, ZIF-8 is able to serve as a microreactor where foreign metal atoms, from either ionic salts or covalent molecules, can be stabilized within the framework while remaining spatially separate. In Table 1, we summarize some of the commonly reported fabrication methods of ADMCs based on ZIF-8 precursors. It is noteworthy that these metal introduction methods can be combined to achieve higher metal loading. More importantly, it enables the successful fabrication of several dual-metal sites, as demonstrated by Wang *et al*.[93], Xiao *et al*.[94] and Ren *et al*.[95].

Polymers have a well-defined molecular structure, and a variety of polymers can transform into carbon after treatment at high temperatures in an inert atmosphere with acceptable carbon yield. Thus, polymers may be a rational choice as carbon precursors. However, not all polymers can be utilized as carbon sources for ADMCs. An ideal carbon precursor should have proper carbonization yield, as a yield that is too low will gradually increase the concentration of metal species during the carbonization, which usually leads to aggregation. In addition, the composition and structure of the resultant carbon should be suitable for anchoring ADMs. Similar to the MOF discussed above, achieving heteroatom doping is vital for the fabrication of ADMCs in the case of polymers as well. Thus, those with heteroatoms, especially N atoms, in the polymer chain are more favored, such as polyaniline, polypyrrole, polydopamine, and polyacrylonitrile.

Polyaniline (PANI) and polypyrrole (PPy) are N-rich polymers, sharing similarities in fabrication procedures and molecular structures. Both polymers can be obtained simply by oxidative polymerization of respective monomers by oxidation agents in aqueous media[96,97]. The N atoms within the polymer chain are functional in stabilizing metal species[98] [Figure 5A], and after high-temperature treatment, a considerable amount of N remains within the carbon framework. Some metal ions, such as Fe^{3+}, are oxidative enough to trigger the polymerization of aniline and pyrrole. Li *et al*. demonstrated that by treating $CoFe_2O_4$

Table 1. Methods utilizing ZIF-8 as carbon precursors

Material	Metal precursor	Fabrication system	Interaction	Application	Ref
Fe-N-C-950	$Fe(acac)_3$	Wet-chemical	host-guest	ORR	[83]
Mn-N-C-HCl-800/1100	$MnCl_2$	Wet-chemical	Metal substitution	ORR	[84]
Ce SAS/HPNC	$Ce(NO_3)_3$	Wet-chemical	Metal substitution	ORR	[85]
Ir_1-N/C	$IrCl_3$	Solid-state	Metal substitution	ORR	[86]
Fe2-Z8-C	$Fe(Ac)_2$	Solid-state	Metal substitution	ORR	[87]
Ir-SACs	$Ir(acac)_3$	Wet-chemical	host-guest	ORR	[11]
Fe2-N-C	$Fe_2(CO)_9$	Wet-chemical	host-guest	ORR	[88]
(Fe,Co)/N-C	$Co(NO_3)_2$	Wet-chemical	Metal substitution	ORR	[83]
(Fe,Co)/N-C	$FeCl_3$	Wet-chemical	Adsorption	ORR	[83]
C-AFC@ZIF-8	Ammonium ferric citrate	Wet-chemical	Adsorption	ORR	[89]
FeCo-DACs/NC	FeCo binuclear phthalocyanines	Wet-chemical	host-guest	ORR/ OER	[90]
Co-SA/P in situ	$Co(NO_3)_2$	Wet-chemical	Metal substitution	HER	[91]
Y_1/NC	Y_2O_3	Solid-state	Metal substitution	NRR/ CO_2RR	[92]
Ni_2/NC	$Ni_2(dppm)_2Cl_3$	Wet-chemical	Post adsorption	CO_2RR	[60]
Ni_1/NC	$NiCl_2$	Wet-chemical	Post adsorption	CO_2RR	[61]

nanoparticles in an acid solution containing pyrrole, Fe^{3+} is leached off from $CoFe_2O_4$, starting the polymerization of pyrrole at the surface of nanoparticles[99]. As a result, a hollow PPy shell can be obtained, within which Fe^{3+} and Co^{2+} are bonded. By simple pyrolysis, ADMCs with Fe and Co sites can be obtained [Figure 5B-E][99]. Jin *et al*. reported a simple method to fabricate Fe ADMCs with tunable Fe loading using PPy. The as-prepared PPy hydrogel was immersed in the acholic solution of iron(III) 2,4-pentanedionate with different concentrations before being washed and dried. After pyrolyzed, the PPy chains carbonized into an N-doped carbon framework, obtaining Fe ADMCs[100]. Weng *et al*. suggested that by adding aniline into the clay bank slurry formed by dispersing excessive $FeCl_3$ in ethanol, FePANI can be obtained, which, after thermal treatment and acid washing, transformed into Fe ADMCs[101].

Polydopamine (PDA) has attracted increasing attention as a carbon precursor for its ability to grow outside other substances, duplicating the morphology of the substrate. Zhang *et al*. found that PDA can grow tightly on the surface of various metal oxides/hydroxides, and after high-temperature pyrolysis, a thin layer of carbon with metal ADMs diffused from the inner core can be obtained[102]. Similarly, Han *et al*. demonstrated that PDA can duplicate the cubic morphology of CoNi-based Prussian blue analogs [Figure 5F-I][103]. The novel thin-shelled morphology increases the ratio of surface atoms, benefiting their utilization in catalysis. Zhou *et al*. demonstrated a hierarchical mesoporous carbon sphere with Fe ADMs. The self-polymerization of dopamine on the F127 micelles stabilized by TMB is critical for the formation of such morphology [Figure 5J-K][104]. Thin carbon shells with abundant Co ADMSs were fabricated by Zhang *et al*. utilizing the polymerization of dopamine at the surface of SiO_2 nanoparticles in the presence of cobalt nitride followed by carbonization[105]. As shown in Figure 5L, these carbon shells are extremely thin, with a thickness of less than 5 nm. Ou *et al*. grew PDA on the surface of graphene oxide peeled off from Fe foam, and the sheet-like morphology of GO was entirely duplicated[106].

Polyacrylonitrile (PAN) is another commonly used polymer as a carbon precursor, especially in electrospinning to fabricated ADMCs with fiber-like morphologies. Even though the cyano groups are rich in N content, the research on the thermal behavior of PAN reveals that the massive denitrogenation of PAN starts at 700 °C, making the participation of additional heteroatom precursors necessary in the formation of

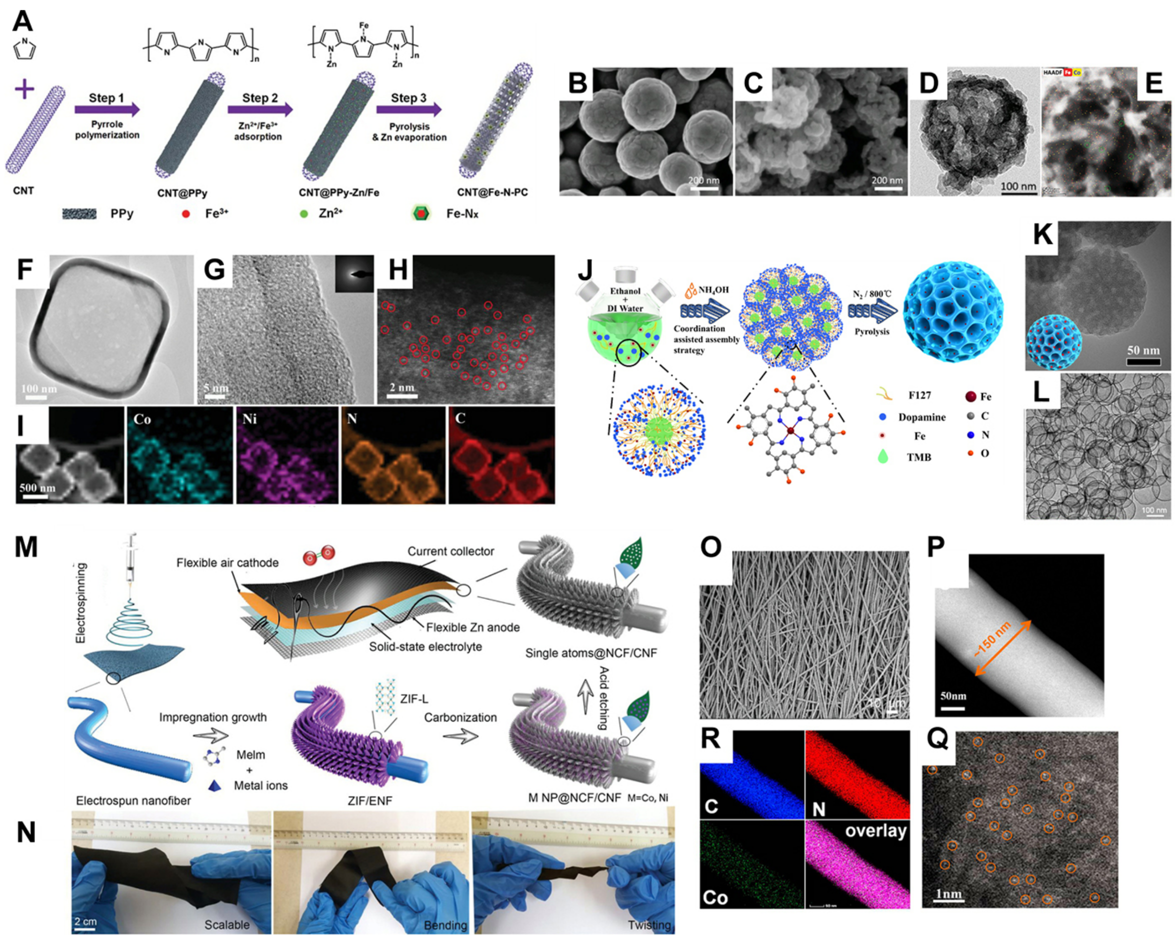

Figure 5. (A) Illustration of the preparation process of CNT@Fe-N-PC via adsorption[98], reproduced from Ref. [98] with permission. Copyright 2018 Springer Nature. (B) SEM images of the $CoFe_2O_4$ sphere, and (C) SEM, (D) TEM, (E) HAADF-STEM images of FeCo-N-HCN[99], reproduced from Ref.[99] with permission. Copyright 2021 Wiley-VCH. (F and G) TEM, (H) aberration-corrected HAADF-STEM images, and (I) EDS element mapping of CoNi-SAs/NC[103], reproduced from Ref.[103] with permission. Copyright 2019 Wiley-VCH. (J) Illustration of the fabrication process of meso-Fe-N-C, and (K) TEM image of meso-Fe-N-C[104], reproduced from Ref.[104] with permission. Copyright 2021 American Chemical Society. (L) TEM image of CoSA/N,S-HCS[105], reproduced from Ref.[105] with permission. Copyright 2020 Wiley-VCH. (M) Illustration of the fabrication process of flexible electrode based on SA@NCF/CNF, (N) digital photos of Co SA@NCF/CNF flexible electrode under rolling, bending, and twisting state, and (O) SEM image of Co SA@NCF/CNF[111], reproduced from Ref.[111] with permission. Copyright 2019 Wiley-VCH. (P) HAADF-STEM image, (Q) EDS element mapping, and (R) aberration-corrected HAADF-STEM image of Co-N/CNFs[112], reproduced from Ref.[112] with permission. Copyright 2017 American Chemical Society.

ADMs. Zhao *et al.* demonstrated the effectiveness of PMMA as an N precursor in the fabrication of Sn ADMCs using electrospinning[107]. Metal macrocyclic compounds such as cobalt porphyrins can be stabilized directly in carbon fiber without additional N sources, as demonstrated by Zhang[108]. Besides contributing to the formation of a carbon framework supporting ADMCs, the PAN-based electrospinning technique is effective in fabricating fiber-like morphologies with other carbon precursors. Yang *et al.* fabricated fiber-like Fe ADMCs doped with S and N. Thiourea and Fe/ZIF-8 were added into the DMF solution of PAN for electrospinning, thiourea and Fe[109]. Cheng *et al.* reported a porous carbon fiber derived from electrospinning of the DMF solution of PAN with SiO_2, which is utilized for the growth of Fe-ZIF-8[110]. A similar procedure was adopted by Ji *et al.* to fabricate Co ADMCs utilized as a flexible electrode, shown in Figure 5M[111]. After pyrolysis, ZIF-8 contributed to the carbon component hosting near ADMs, while PAN contributed to the fiber structure connecting ZIF-8-derived carbon particles. Such a strategy is able to combine the advantages of ZIF-8 and PAN as carbon precursors, creating a loosely-arranged flexible carbon matrix with better mass transport channels [Figure 5N and O]. In Yang's report, by pyrolyzing the fiber fabricated by electrospinning the DMF solution of 4-dimethylamino-pyridine, cobalt acetate, and PAN, Co-based ADMCs can be obtained. The resultant has a uniform fiber-like morphology with abundant Co ADMs [Figure 5P-R][112].

The conversion of biomass into functional materials, including ADMCs, has long been of interest. This biomass contains proteins, carbohydrates, lipids, and other organic components, which release a large amount of gas when treated at high temperatures, contributing to the formation of micropores. Zhang *et al.* reported that by pyrolyzing cattle bone, a hierarchically structured porous carbon with N- and O-containing functional groups and numerous micropores can be obtained. Such carbon material has a specific surface area as large as 2,540 m^2g^{-1}, which is suitable for anchoring ADMs[113]. As reported by Zhang *et al.*, porphyra was carbonized and activated by KOH, forming a carbon support, into which hemin was added. After high-temperature pyrolysis, Fe ADMCs with Fe loading of 2.3 wt.% can be obtained[114]. Wang *et al.* used silk as a carbon precursor to fabricate Fe ADMCs without the addition of a heteroatom precursor. Silk consists largely of protein, where plenty of amino groups exist. These amino groups are able to bond metal ions, facilitating the formation of ADMCs[115].

Simple organic molecules, such as dicyandiamide[116], melamine[117,118], glucosamine[119], amino acids[120], glucose[121,122], chitosan[123,124], EDTA[125], can also be utilized as carbon precursors. Some of the N-containing molecules can also serve as heteroatom precursors at the same time.

Carbon or its derivatives as carbon precursors

Instead of obtaining carbon from the carbonization of organics, various carbon materials or carbon derivatives have been utilized as carbon precursors for ADMCs: carbon black, graphite, graphene oxide, carbon nanotubes, carbon nanofibers, and graphene.

Different from other organics, the structure of carbon is relatively stable and does not undergo severe reconstruction in thermal treatment. Thus, it is doubtful whether the carbon structure participates in the formation of the local structure of ADMs. In some other reports, defects in carbon are able to serve as ligands and directly stabilize ADMs without heteroatom doping. Liu *et al.* demonstrated that by pyrolyzing platinum acetylacetonate with defective carbon black pre-treated in hydrogen peroxide, Pt atoms can be anchored at the divacancies by four carbon atoms in the form of PtC_4[126]. This phenomenon further highlights a common principle in the formation of ADMs: strong chemical interaction between ADMs and the support. Should there be suitable anchoring points (such as carbon vacancies), ADMs can form on carbon even without additional heteroatom dopants[127].

The heteroatoms can be introduced via a second precursor during pyrolysis or by surface functionalization in a pre-pyrolysis step. The surface chemical composition of carbon can be easily regulated by various functionalization reactions. After surface functionalization by concentrated nitric acid, the oxygen-containing functional groups are able to bind Co atoms to form CoN_2O_2 ADMS[128]. These carbonaceous components not only serve directly as anchoring substrates for ADMs but can also act as diluents that increase the dispersion of other carbon precursors or as electron conductors that facilitate charge transfer.

Carbon black, including XC-72, Ketjenblack, Black Pearls and *et al.*, have partially graphitic moieties together with defects. The pore structure varies with the type of carbon black. The microporous structure of carbon black benefits the adsorption of heteroatom/metal precursor and the formation of ADMs in later pyrolysis. As reported by Yang *et al*., by evaporating the dispersion of carbon black, metal chloride/nitride, and 1,10-phenanthroline monohydrate, a black powder with uniformly distributed metal ions can be obtained, which after a mild thermal treatment at 600 °C, transform into atomically dispersed metal sites (ADMSs) with well-defined single atom structure[129], shown in Figure 6A. It is suggested that such a method is feasible to fabricate Ni ADMCs with Ni loading varying from 2.5 to 5.3 wt.% [Figure 6B-E], and due to the controllable procedure and commercial availability of carbon black, it is able to produce at a large scale [Figure 6F]. Xie *et al*. demonstrated a post-formation procedure using carbon black as a carbon precursor. Upon adsorbing Cu species in a concentrated ammonia solution with dissolved CuCl and thermal treatment at 500 °C, Cu ADMs can be formed, shown in Figure 6G and H[130]. Wang *et al*. demonstrated Ni ADMCs prepared by simple pyrolyzing oxidized carbon black decorated with Ni-containing complex[131].

Graphene and carbon nanotubes are carbon allotropes composed of sp^2 hybridized carbon with hexagonal-arranged structures. Unlike carbon black, ideal graphene and carbon nanotube are highly crystallized with few defects. Strictly speaking, graphene is a single-layer graphite sheet. However, in the booming of research since its discovery, few-layered graphite sheets are sometimes referred to as graphene as well. Graphite has a highly-ordered structure with satisfying electron conductivity. In some cases, graphite powder serves directly as a carbon precursor undergoing ball-milling with metal macrocyclic compounds when the adsorbed molecules gradually become connected to the surface of graphite particles, becoming ADMCs, as shown in Figure 6I-K[52]. However, due to the stacked layer in graphite not favoring the full exposure of the carbon surface for the anchoring of ADMs, graphene with single or few layered carbon sheets is considered more suitable and qualified as carbon precursors.

In most cases, instead of graphene itself, graphene oxide, as a carbon derivative, is utilized based on the following considerations. For one, graphene oxide comes from successive oxidation, intercalation, and exfoliation of graphite, which is rather feasible on a lab scale. For another, due to the abundant oxygen-containing functional groups on graphene, it can be well dispersed in an aqueous solution easily, making it possible to form composites with other substances or construct unique morphology. These functional groups on graphene are removed during high-temperature pyrolysis, recovering the crystalline structure and conductivity of graphene.

Despite the seeming advantages of graphene, it is not easy to construct graphene-based ADMCs using all solid thermal reactions. First, graphene sheets have a high tendency to restack at elevated temperatures, especially when surface oxygen-containing functional groups are removed. Second, the rearrangement of atoms during pyrolysis is minor, with detaching of O-containing functional groups, shown in Figure 6L, much different from the complete rearrangement on other organics, which favors the embedding of ADMs[132], and the surface of graphene lacks micropores where ADMs favor to locate. As a result, the use of graphene oxide as carbon precursors is limited. If the pyrolysis temperature is low enough to maintain some of the oxygen-containing functional groups, O atoms are able to stabilize ADMs by O coordination. Gao *et al*. demonstrated Co ADMs stabilized by O atoms on graphene sheets[133]. By freeze-drying the dilute solution of $CoCl_2$ with graphene oxide, it is believed that Co^{2+} ions can form stable bonds with surface O-containing functional groups. after a mild thermal treatment at 550 °C, these adsorbed Co atoms are stabilized[133]. A similar procedure was reported by Liang *et al*., and before the adsorption of organic Ti salt, GO was first treated with ozone to introduce more O dopants as well as vacancy defects for the anchoring of Ti atoms[134]. By pyrolyzing the mixture of pre-treated GO with Ti salt adsorbed at 550 °C, Ti-based ADMCs can be obtained with a TiO_4OH coordination structure [Figure 6M-O][134]. Fei *et al*. reported microwave-assisted methods to fabricate Co ADMs on graphene. The GO precursor doped with N through hydrothermal reaction with ammonia solution was mixed with $CoCl_2$ and freeze-dried. After being treated

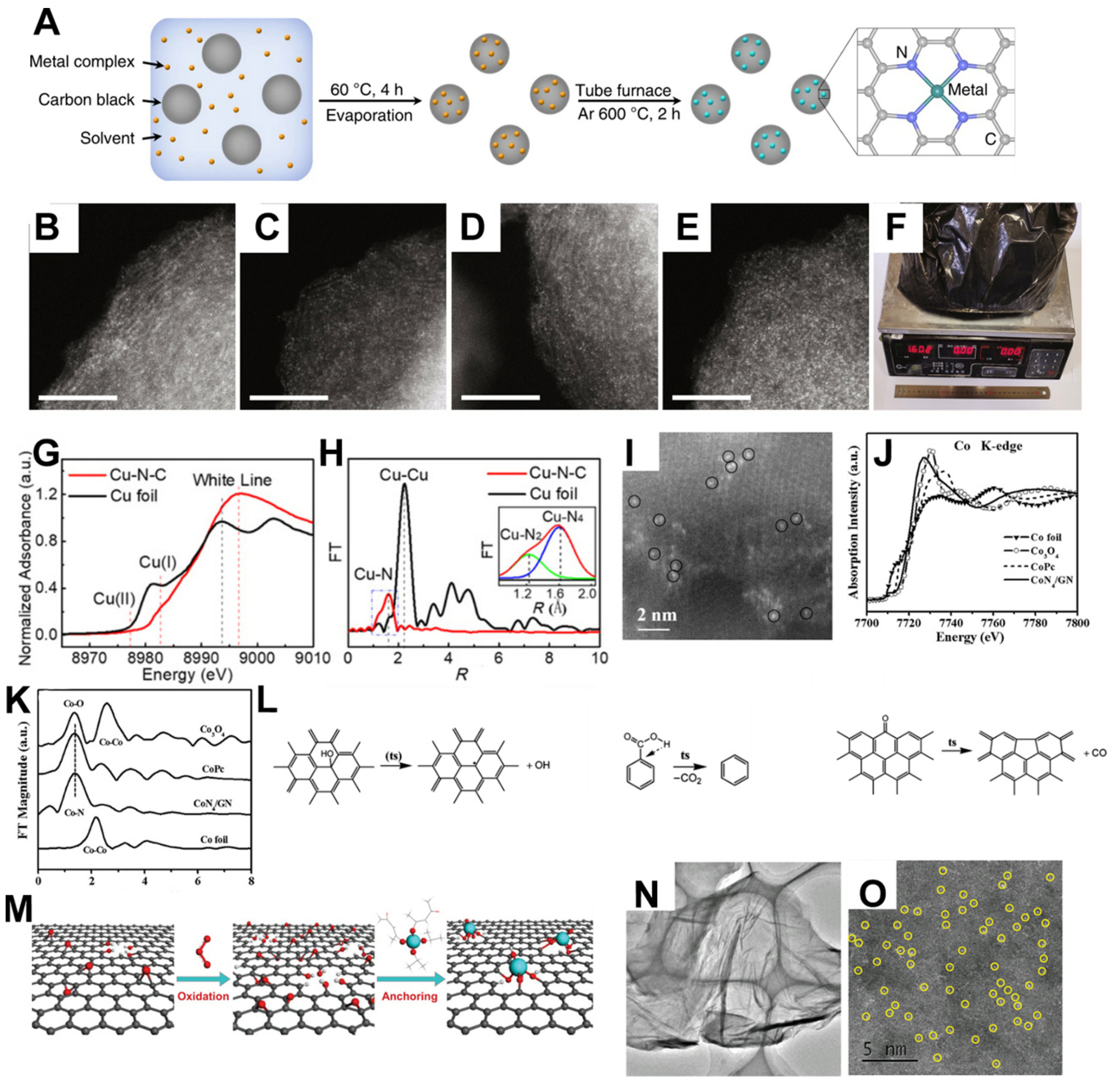

Figure 6. (A) Illustration of the universal procedure to produce ADMCs, (B-E) aberration-corrected HAADF-STEM image for Ni-SAC with Ni loading of 2.5, 3.4, 4.5, and 5.3 wt.%, respectively, and (F) photograph for Ni-SAC-2.5 synthesized in large scale[129], reproduced from Ref.[129] with permission. Copyright 2019 Springer Nature. Cu K-edge (G) XANES, and (H) EXAFS spectra of Cu-N-C[130], reproduced from Ref.[130] with permission. Copyright 2018 Wiley-VCH. Aberration-corrected (I) TEM, (J) Co K-edge XANES and (K) EXAFS spectra of CoN_4/GN with other Ref.[52], reproduced from Ref.[52] with permission. Copyright 2016 Wiley-VCH (L) Illustration of the thermal reduction reaction of graphene oxide[132], reproduced from Ref.[132] with permission. Copyright 2010 American Chemical Society. (M) Illustration of the synthesis of Ti_1/rGO, (N) TEM and (O) aberration-corrected HAADF-STEM images of Ti_1/rGO[134], reproduced from Ref.[134] with permission. Copyright 2020 Wiley-VCH.

in a microwave oven for 5 s, the solid mixture transformed into Co ADMs can be obtained. Ni ADMCs can be obtained as well using a similar procedure[135].

One effective protocol to stabilize embedded ADMs with N coordination on graphene involves highly reactive gas, which will be introduced in Section "FIXATION VIA LIGAND REPLACEMENT". The condition is similar to carbon nanotubes as well.

Heteroatom/Metal precursor and pyrolysis parameter

As stated above, most users reported ADMs to have non-carbon heteroatoms as anchoring points for metal atoms; thus, a heteroatom precursor is needed. For those MOFs or polymers with heteroatoms within the molecular structure, a second precursor can be omitted. For example, most ZIF-8 precursors with pre-existing M-N bonds for MNx ADMs and MIL-88(Al) MOF with pre-existing Al-O bonds for Al-O ADMs[68].

The N precursors can be N-rich organics, including amines, urea, or inorganics, such as ammonium salt, similar to N-doping of carbon. There is evidence that the ammonia produced by precursor decomposition at elevated temperatures is the key ingredient for the formation of ADMs. Besides N, nonmetal elements such as B, S, O, and P introduced into the carbon can participate in the coordination of metal atoms as well.

As for the metal precursors, even though simple metal salts are capable of fabricating ADMs, it is believed that the existing M-N bond in the precursors is beneficial for the formation of ADMs, probably due to simplified atomic rearrangement, making it easier and faster to inherit the original coordination in the precursors. This is exactly true for the scenarios when metal macrocyclic compounds and other metal precursors with N coordination are used.

The pyrolysis temperatures have an enormous impact on the chemical composition and structure of the products produced since not only the formation of ADMs is temperature-dependent, but also the carbonization of organics and the development of the structure and composition of the carbon skeleton are strongly dependent on temperature. Thus, the nature of precursors should be taken into consideration when deciding the pyrolysis parameters. Generally speaking, if the stabilization of metal atoms is achieved by the functional groups on carbon, a lower pyrolysis temperature should be chosen compared with those with additional heteroatom precursors. The *in-situ* formation of embedded ADMs out of simple metal salt requires a higher temperature than using macrocyclic compounds or biomolecules with well-defined M-N coordination. The decomposition temperature of the metal salt is also vital, as revealed by Wan *et al*. that the usage of metal chlorides or nitrides has brought tremendous differences in the composition of the final product[136].

The temperature chosen is determined mainly by the targeted structure of the product. Generally speaking, raising pyrolysis temperatures results in higher graphitic degrees and fewer heteroatoms within the carbon framework, which is beneficial for improving conductivity and electrochemical stability, but destabilizes some ADMs in the meantime. It is comprehensible that for purposes other than the electrochemical field, the electron conductivity need not considering, and the pyrolysis condition can be as mild as below 600 °C[77,125,134]. In the case of MOF-based methodologies, higher temperatures above 800 °C are always favored. In some cases, in order to promote the graphitic level of carbon framework, aiming at promoting the resistance against chemical and electrochemical corrosion, temperatures as high as 1,100 °C were adopted[87,137]. According to Hai *et al*. and Wang *et al*., the coordination environment of CoN_4 moieties gradually transforms into CoN_2C_2 when elevating pyrolysis temperatures from 800 to 1,000 °C[44,45]. A similar phenomenon is observed on Fe ADMCs as well[46]. Even though the replacement of N with C does not necessarily result in the instability of ADMs, other publications suggest that overly high temperature reduces the amount of metal-stabilized as ADMs due to possible aggregation[138].

FIXATION VIA LIGAND REPLACEMENT

Research on the formation mechanism

With the successful demonstration of several newly emerged fabrication methodologies, evidence appeared that the formation of ADMs can be achieved via direct fixation of gas species via ligand replacement, similar to the phenomenon observed in the wet-chemical reaction[43].

Such a mechanism is typical for systems with the gas-phase introduction of key species. For instance, Wang *et al*. suggested that the formation mechanism of Co ADMCs via a noncontact gas-migration-trapping strategy using $CoCl_2$ as a metal precursor is that the precursor placed in a separated boat first sublimates and is then trapped, reduced, and stabilized in the N-doped carbon framework in the form of single atoms[21]. Hai *et al*. suggested that the fixation of metal atoms from gaseous chloride into N_4 vacancies proceeds via two endothermic and one spontaneous ligand replacement steps, releasing HCl, and is thermodynamically favored overall [Figure 7A][61]. Using a two-step pyrolysis procedure, they were able to identify the intermediate state with both Ni-N bonding and Ni-Cl coordination by EXAFS spectra on the Ni K-edge [Figure 7B].

Other attempts highlighted the importance of N precursors in the formation of gaseous metal species and their fixation, and it is inferred that these ADMs are formed via ligand replacement as well. Ou *et al*. suggested that with the help of ammonia at high temperatures, metallic Cu is able to release $Cu(NH_3)_x$ species based on strong Lewis acid-base interactions, which can diffuse and then be trapped by defects of the carbon substrate, forming Cu ADMs[139]. Based on a similar process, Co and Ni can also be introduced from bulk metals. Ou *et al*. suggested that it is the ammonia generated by the decomposition of dicyandiamide that contributes to the emission of Pt atoms from bulk Pt [Figure 7C][140].

Different from the abovementioned mechanism, as demonstrated by Jiao *et al*., the gaseous metal salt can not only be captured by proper vacancies forming ADMs but also react with existing moieties and replace the metal center [Figure 7D][141]. By introducing $FeCl_3$ into a fully carbonized ZIF-8, the original Zn-N_4 moieties are transformed into Fe-N_4 according to the following equation:

$$FeCl_3 + Zn\text{-}N_4 + X = Fe\text{-}N_4 + ZnCl_2 + XCl$$

Such a mechanism is supported by mass spectrometry with an intense signal assigned to HCl and $ZnCl_2$ during thermal treatment [Figure 7E and F][141].

Applicable scenario

With the experimental observation of the traditional all-solid procedures, the nature of the complicated thermal reactions is partially uncovered, with evidence of the substance contributing the most to the formation of ADMs. With such knowledge, new procedures with stronger pertinency and higher efficiency have been developed. In this section, the thermal reaction involving active gaseous species is introduced.

Gas-phase introduction of key nonmetal species

Despite the fact that there is always gas evolution during the thermal treatment of organics in the all-solid reactions described above, some other procedures have unique features in that the key nonmetal species are introduced directly from additional cylinders or originate from the compound placed in a separate vessel in the furnace without direct contact with the carbon source. On the one hand, these procedures prove the important role played by these gaseous nonmetallic species. On the other hand, they save researchers the trouble of possible purification when the origin of these species is mixed with the main product, as is the case with all the solid reactions mentioned above.

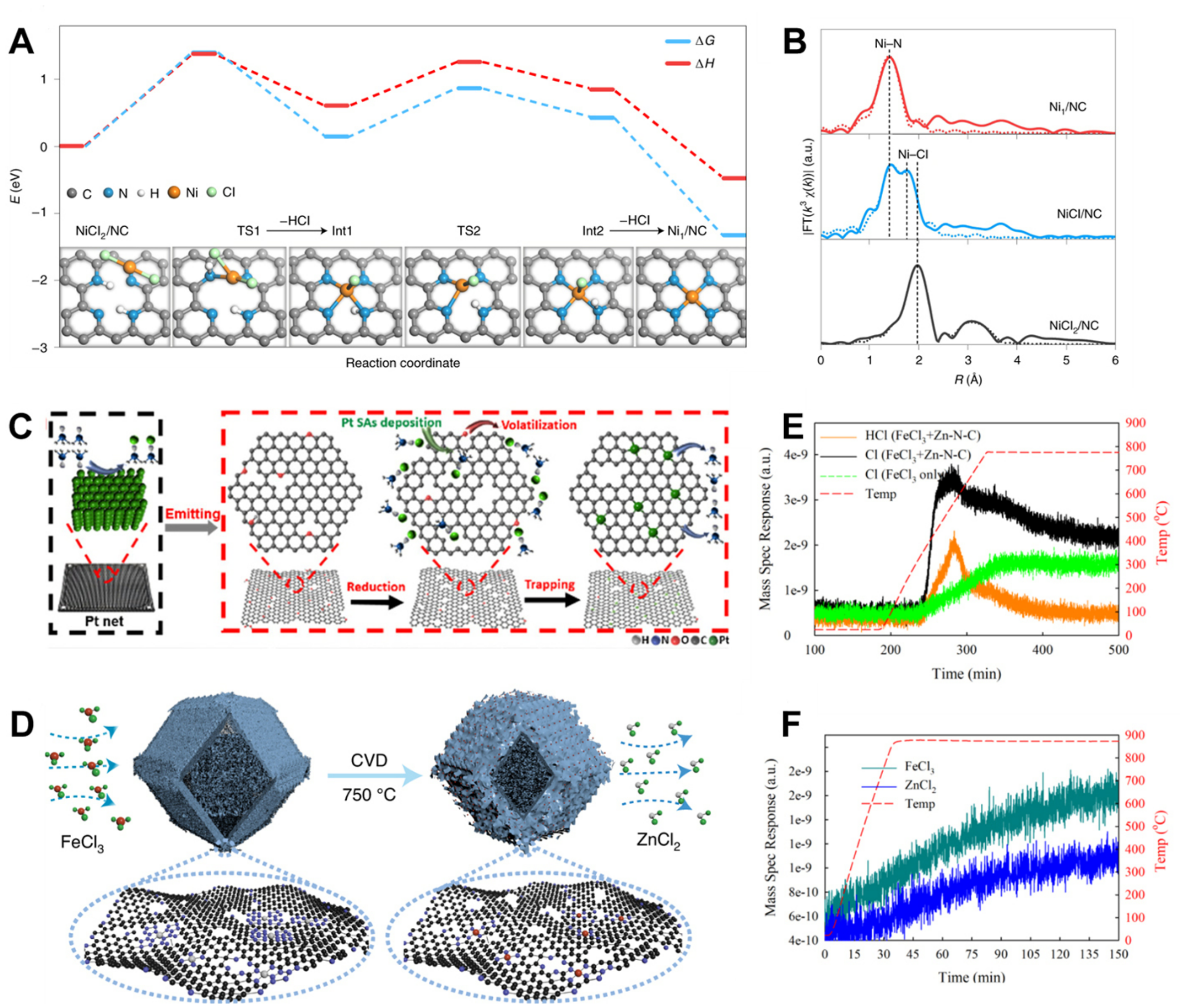

Figure 7. (A) DFT-calculated energy pathway for the formation of Ni-N_4 from the $NiCl_2$ and (B) Ni K-edge EXAFS spectra of $NiCl_2$/NC precursor, NiCl/NC intermediate, and Ni_1/NC[61], reproduced from Ref.[61] with permission. Copyright 2021 Springer Nature. (C) Illustration of the formation process of Pt ADMS using thermal emitting[140], reproduced from Ref.[140] with permission. Copyright 2019 American Chemical Society. (D) Illustration of the formation process of Fe ADMS from metal center replacement, (E and F) TG-MS signals revealing the gas emission[141] during metal center replacement, reproduced from Ref.[141] with permission. Copyright 2021 Springer Nature.

Up to now, ammonia has been proven the most effective in promoting the atomization of metal species. The detailed mechanism is not yet understood, and it is speculated that NH_3 plays an important role in the production of metal-containing gaseous species, which can easily be fixed within the carbon framework[139]. At the same time, the reaction between ammonia and carbon creates micropores and dopes N into the framework, which also benefits the fixation of ADMs[142]. Such effects are so strong that they can reverse the metal aggregation at elevated temperatures, making some of the less favored systems, GO and CNT, for example, capable of producing ADMs. Even though graphene has a huge surface area, it is not a qualified carbon substrate due to the accessible micropore structure being insufficient to host a large number of ADMs. This situation is more apparent when using graphene oxide as support. During the thermal treatment of graphene oxide, the rearrangement of carbon atoms is not thoroughly compared with the carbonization of organics, resulting in little chance of fixing ADMs. Thus, direct pyrolysis of graphene oxide with metal precursors and solid metal dopants usually ended up with metal aggregates. With the help of ammonia, various metal elements can be fixed onto the carbon framework with MN_x coordination, and in those cases, a second solid N precursor is not necessary [Figure 8A and B][121,143-146]. In other procedures, it is believed that the N-containing active gas, ammonia, for example, is responsible for the formation of metal-containing species and the formation of ADMs on carbon. Our group obtained Cu ADMCs based on a high-temperature procedure where the mixture of carbon derivatives (graphene oxide, functionalized CNT, or active carbon) and dicyandiamide are placed in a capping boat wrapped tightly by Cu foil. They believe that the participation of the decomposition product of dicyandiamide in the formation of reactive Cu-containing species [Figure 8C-E][147].

In addition to promoting the atomization of metal elements, it has been reported that ammonia treatment has tremendous effects on the coordination structure of ADMs. According to Zhang *et al*., compared with Ar, Fe ADMCs fabricated in ammonia have a regulated second coordination shell, converting the original pyridinic N for the anchoring of Fe atoms into pyrrolic type while maintaining the original FeN_4 first coordination shell [Figure 8F and G][12].

Very recently, the utilization of HCl derived from ammonia chloride has also proven effective in downsizing metal aggregates into ADMs. Li *et al*. reported that by thermally treating a mixture of ZIF-8 derived carbon with nanosized Fe powder and ammonia chloride at 500 °C, with the help of reactive gaseous hydrogen chloride and ammonia, metal aggregates can be converted entirely into ADMs [Figure 8H][148].

Gas-phase transfer of metal species

In addition to regular solid metal precursors, some metal precursors can be introduced via gas-phase transfer. Compared with solid mixing, an apparent advantage of doing so is the higher dispersion of the metal precursor in the gas phase, guaranteeing the uniform mixing of the metal precursor and carbon substrate. Another advantage is that only surfaces with sufficient gas-diffusion pathways can serve as anchoring points for ADMs, facilitating their utilization, especially in catalysis.

Metal precursors can be volatile metal salts, such as metal chlorides and acetylacetonates with lower boiling points, which evaporate as the temperature rises and then make contact with the carbon precursor.

Wang *et al*. developed a noncontact gas-migration-trapping strategy using $CoCl_2$ as a metal precursor to form Co-based ADMs on carbon placed in a separated boat during pyrolysis[21]. Jiao *et al*. demonstrated a similar procedure with the gaseous introduction of $FeCl_3$, obtaining Fe-N_4 moieties within the carbon framework placed in a separate boat[141]. Hai *et al*. suggested that by introducing gaseous chloride molecules into the chamber where substrate materials exist and performing two thermal treatments spirited by a washing step, a high loading level of metal can be achieved on carbon [Figure 8I][61]. This procedure showed remarkable universality, with 15 metal elements being able to be fixed in the form of ADMs.

In other reports, metal is introduced from metal bulk or involatile oxide with or without the assistance of gaseous N-containing species, depending on the procedure. Han *et al*. developed a novel self-initiated dispersing protocol, proven effective in fabricating Cu-based ADMCs out of metallic Cu with the help of dicyandiamide within a quasi-enclosed system[147]. Because the metal source and carbon substrate were not in contact, the appearance of Cu ADMs on the carbon substrate clearly indicated the gaseous transfer of the Cu source. Ou *et al*. demonstrated a method using bulk metal as a source, which introduces Cu/Co/Ni ADMs into carbon via gas-phase transfer with the help of ammonia at high temperatures[139]. Ou *et al*. reported that using Pt mesh and dicyandiamide, Pt ADMs formed on carbon via noncontact pyrolysis[140].

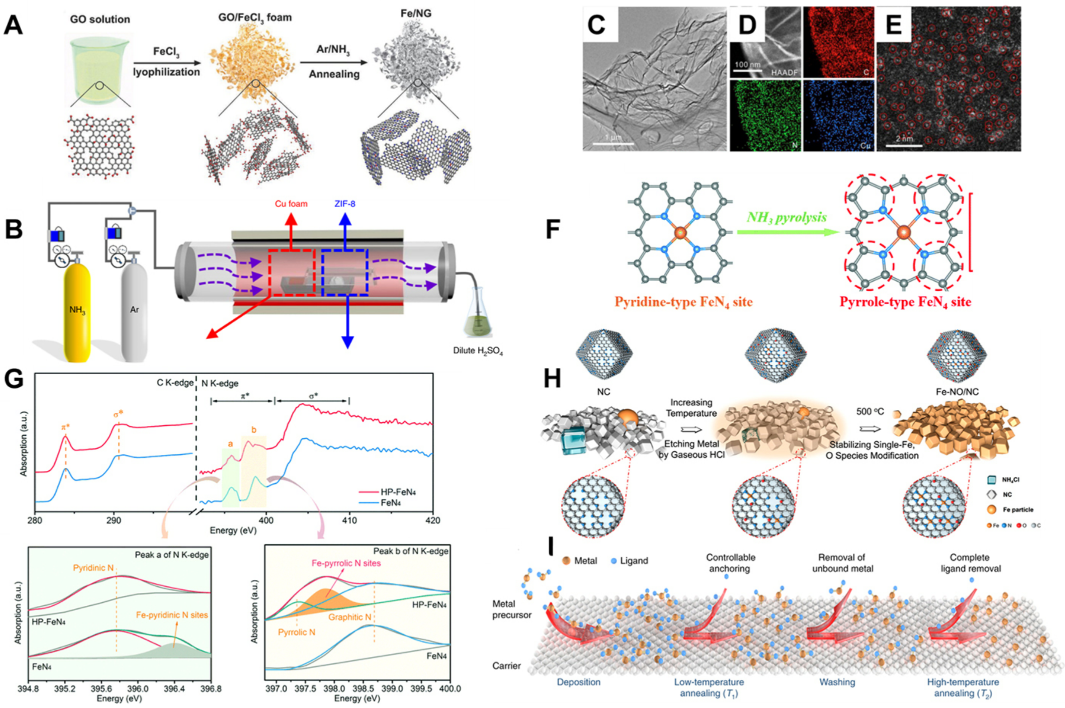

Figure 8. (A) Illustration of the ammonia-assisted fabrication process of Fe/NG[146], reproduced from Ref.[146] with permission. Copyright 2018 Wiley-VCH. (B) Illustration of the ammonia-assisted fabrication process of Cu ADMCs[140], reproduced from Ref.[140] with permission. Copyright 2019 American Chemical Society. (C) TEM, (D) EDS element mapping, and (E) aberration-corrected HAADF-STEM images of Cu-G[147], reproduced from Ref.[147] with permission. Copyright 2019 Elsevier. (F) Illustration of the transformation of pyridinic FeN_4 to pyrrolic FeN_4 by ammonia treatment, and (G) C K-edge and N K-edge XANES spectra od HP-FeN_4 and FeN_4[12], reproduced from Ref.[12] with permission. Copyright 2020 Royal Society of Chemistry. (H) Illustration of the fabrication process of Fe-NO/NC assisted by NH_4Cl[148], reproduced from Ref.[148] with permission. Copyright 2020 American Chemical Society. (I) Illustration of a universal two-step method for the fabrication of ADMCs[61], reproduced from Ref.[61] with permission. Copyright 2021 Springer Nature.

DIRECT ANCHORING

As the all-solid procedures are the major procedure for the fabrication of ADMCs, several mechanisms via solid-solid interactions have been proposed based on direct observation or indirect speculation. It is suggested that active metal atoms may be emitted from the bulk, which are then captured by the proper vacancies, forming ADMCs. The entire reaction can occur at the interface of the metal source and substrate or in noncontact situations.

The formation of ADMCs at the interface of the metal source and substrate requires the diffusion of metal atoms from the bulk metal source and their fixation within the substrate. In fact, the phenomenon of solid-state metal diffusion occurring in the contact area of two metals was discovered a long time ago, and the diffusion of metal atoms into the carbon was observed for graphene or carbon nanotubes fabricated by CVD under the catalysis of transition metal nanoparticles[149,150]. However, the single metal atoms within the carbon lattice without proper anchoring points were much less stable than those in the metal lattice. It is believed that creating vacancies (usually single or dual vacancies) is efficient in improving the stability of metal atoms on carbon substrates, which can be further elevated by introducing heteroatoms such as N, S, or P as anchoring points for the formation of ADMCs[127], similar to the phenomena described in the above two sections.

Zhang *et al*. reported that by wrapping various metal oxide/hydroxide particles with polydopamine followed by high-temperature pyrolysis, MN_x moieties can be formed on the outer carbon shells[102]. Such a strategy is effective in fabricating ADMCs with Fe, Co, Ni, Mn, FeCo, FeNi, *et al*. It is believed that the metal oxide/hydroxide at the interface is first reduced by carbon at elevated temperature into a thin layer of metal, during which time there is a strong interaction between metal atoms and the substrate. As a result, when the inner core is removed with acid, stable ADMs are left on the surface of the carbon. It has been shown that polyaniline and polypyrrole with abundant N are also capable of stabilizing metal atoms from the inner core. In the case of ultrasmall metal aggregates, as in the case of nanoparticles, it is possible for these nanoparticles to transform entirely into ADMs. Liu *et al*. suggested that Fe-, Co-, Ni-, and Mn-based ADMCs can be obtained by thermal atomization of the corresponding metal oxide assisted by O-rich graphene oxide and a polymer coating layer[151]. These results highlight the importance of heteroatoms in the carbon substrate.

Such a mechanism receives strong support from the in-temperature identical location transmission electron microscopy (IL-TEM) observation on several systems containing metal nanoparticles. IL-TEM is a powerful tool for observing the changes of material in a selected area as temperature and atmosphere change. Wei *et al*. have observed the atomization of precious metal nanoparticles using IL-TEM[152]. By adding metal nanoparticles into the system where ZIF-8 was synthesized, some can be buried entirely within the ZIF-8 particles. Then a single ZIF-8 particle was traced at a temperature ranging from 100 to 1,000 °C under Ar protection. It is clear from the TEM images that the Pd particles steadily grew larger as the temperature rose to 900 °C due to aggregation. Interestingly, when the temperatures rose up to 1,000 °C, some less aggregated nanoparticles vanished. The aggregation and atomization of Pd lasted for 162 s at 1,000 °C before they completely vanished [Figure 9A and B]. It is believed that Pd atoms are emitted from Pd nanoparticles due to the relatively low vapor pressure of the ultrafine particles at high temperatures and then captured by N-containing defects on the carbon substrate. Similar phenomena were observed on Pt and Au nanoparticles as well.

It is observed that during the process, these particles moved disorderly and collided intensively within the ZIF-8 and the derived carbon particles. It is then inferred that the thermal motion of Pd within ZIF-8 is necessary for its atomization, considering the saturation of anchoring points within a small area and the suppressed emission of larger metal particles. Such a hypothesis is supported by the failure of atomization of Pd on the surface of the ZIF-8 particle, in which case Pd particles were unable to move into the ZIF-8 particle. Thus, it is believed that the evolution of Pd nanoparticle into single atoms are driven by the two competitive processes of atomization and agglomeration, represented by the competitive bonding between Pd-N and Pd-Pd. Using DFT, it is proven exothermic to move a single Pd atom from a cluster to a nearby N_4 vacancy, forming Pd-N_4 ADMs with a large exothermicity of 3.96 eV and an energy barrier of 1.47 eV. In comparison, the aggregation of two Pd atoms is also exothermic, with a small energy barrier of 0.58 eV, shown in Figure 9C. As a result, sintering is the major process at a lower temperature, and when the temperature is high enough, atomization is thermodynamically favored.

In another demonstration by Yang *et al*., Ni nanoparticles acted similarly to precious metals in the above work, i.e., aggregated and then atomized[153]. Because the loading of these particles on the surface of ZIF-8 and the N-containing defects was not sufficient, the atomization was not complete, and a certain content of particles remained. When observing Ni particles loaded on N-free XC-72 carbon black, only aggregation was witnessed, highlighting the importance of N on the atomization of metal particles. However, Qiu *et al*. reported that the CVD process using precursors without N on a porous Ni substrate obtained Ni-based ADMs with NiC_3 configuration[154]. Thus, it is highly likely that despite similar so-called carbon substrates, the detailed structures varied depending on the precursor and thermal treatment parameters.

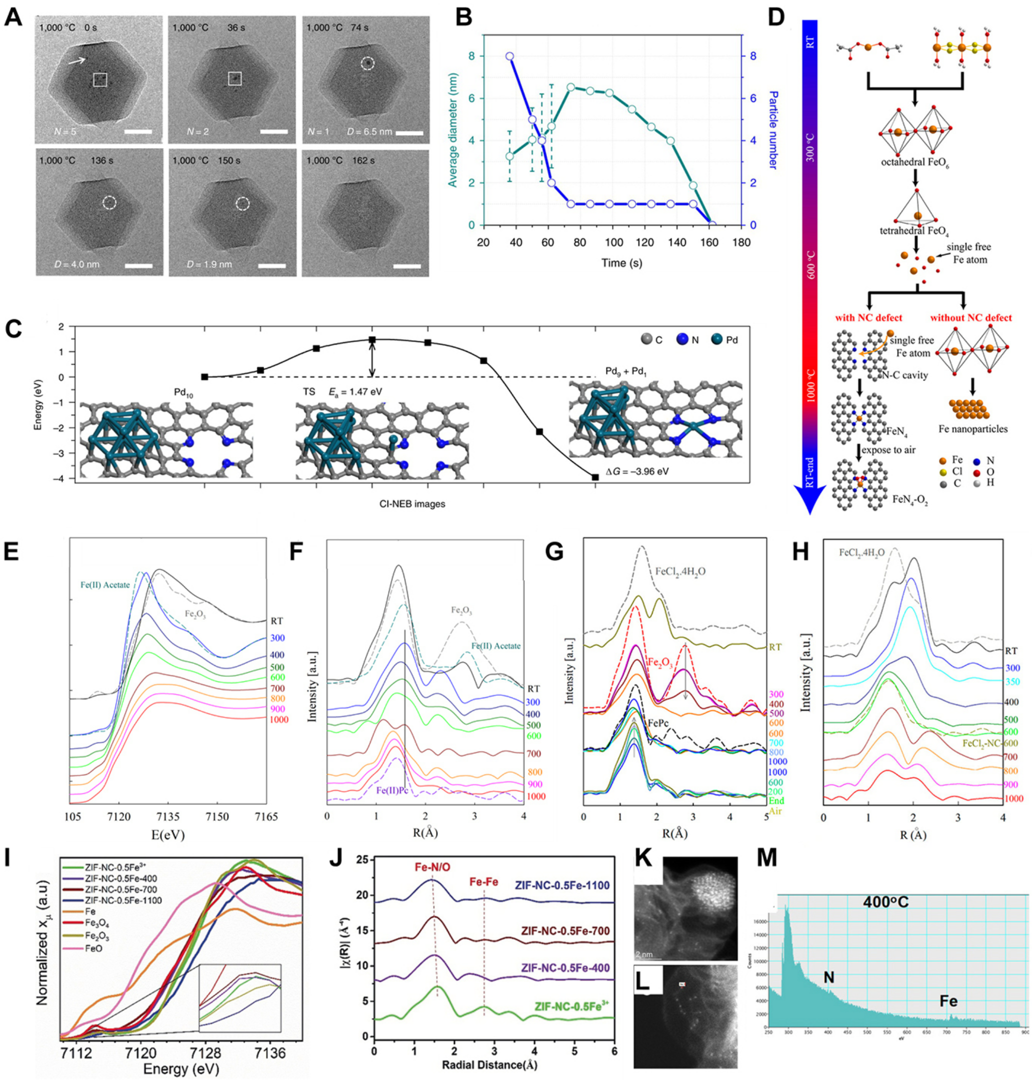

Figure 9. (A) *In-situ* TEM observation, and (B) average number and diameter of Pd particles observed on Pd@ZIF-8 pyrolyzed at 1000 °C for a different time, (C) calculated energy diagram along reaction pathway from Pd cluster to PdN_4[152], reproduced from Ref.[152] with permission. Copyright 2018 Springer Nature. (D) Proposed evolution pathway of $Fe(Ac)_2$ and $FeCl_2·4H_2O$ during thermal treatment, in-temperature Fe K-edge (E)XANES, and (F) EXAFS spectra of the mixture containing $Fe(Ac)_2$, ZIF-8 and 1,10-phenanthroline monohydrate, (G) in-temperature Fe K-edge EXAFS spectra of the mixture of $FeCl_2·4H_2O$ with (G) carbonized ZIF-8, and (H) SiO_2[155], reproduced from Ref.[155] with permission. Copyright 2020 American Chemical Society. Fe K-edge (I) XANES and (J) EXAFS spectra of ZIF-8-NC-0.5Fe pyrolyzed at different temperatures, HAADF-STEM images of (K) ZIF-8-NC-0.5Fe and (L) ZIF-8-NC-0.5Fe-400, (M) EDS spectrum acquired at the marked area in (L)[49], reproduced from Ref.[49] with permission. Copyright 2019 Wiley-VCH.

From the abovementioned information, the following rules relating to the atomization of metal particles into ADMs can be summarized.

1. The formation of ADMs at the interface of metal particles and carbon is thermodynamically favored, and the temperature should be high enough to provide energy to overcome the activation barrier[152].

2. The atomization of metal is achieved by N-containing defects or defects with other forms that can stabilize ADMs[127].

3. The atomization has a saturation level and once reached, the atomization is suppressed[152].

One of the very first attempts to employ the in-temperature XAS technique to investigate the changes in simple Fe salt during high-temperature pyrolysis was made by Li *et al.*[155]. It was proposed that single Fe atoms can be emitted from tetrahedral Fe-O_4 and become Fe-N_4, as illustrated in Figure 9D. The information obtained on several Fe-containing systems was critical to uncovering the evolution of the local coordination environment of Fe as the temperature rises. As demonstrated in the in-temperature Fe K-edge XANES and EXAFS spectra in Figure 9E and F evidence has pictured a clear transition pathway of Fe in the mixture of $Fe(ac)_2$, 1,10-phenanthroline monohydrate and ZIF-8, a commonly seen all-solid system, from the original $Fe(ac)_2$ to Fe-N_4 via Fe_2O_3, FeO with octahedral Fe-O_6 and tetrahedral Fe-O_4. The carbonization process of ZIF does not affect the results, and the transition of tetrahedral Fe-O_4 to in-plane Fe-N_4 is irreversible, while the formation of Fe-N_4 is thermodynamically favored, as shown in Figure 9G. It is then hypothesized after comparing the third systems containing $FeCl_2 \cdot 4H_2O$ and SiO_2 that as O is gradually removed from tetrahedral Fe-O_4, single Fe atoms are formed, which, if captured by nearby N, become Fe-N_4, or otherwise aggregate into metallic Fe [Figure 9H], as illustrated in Figure 9D. The as-formed FeN_4 moieties have satisfying stability due to the high bonding energy of Fe with the N_4 vacancies[127]. As a result, the high diffusion barrier of Fe prevents further aggregation of Fe atoms.

However, as suggested by Li *et al.*, ADMs can be formed directly from iron oxide nanoparticles at temperatures as low as 400 °C, much lower than 600 °C for the formation of active Fe via removal of the lattice O[49]. According to their studies, most of the Fe^{3+} ions adsorbed on N-doped carbon derived from ZIF-8 transform into ultrafine iron oxide nanoparticles upon drying and exposure to air, as evidenced by XAS [Figure 9I and J]. Once treated at 400 °C, these nanoparticles disappeared [Figure 9K and L], and the EELS spectra with high spatial resolution in Figure 9M suggested the formation of FeN coordination, which was in line with the XAS results. DFT calculations also revealed that even though it was energetically unfavorable to remove Fe ions from bulk FeO_x, once captured by pre-existing N_4 vacancies, the entire process became highly exothermic.

Thus, it was concluded that the fixation of metals from simple salts such as chlorides and acetates may not be as simple as once thought. An intermediate state of unstable metal oxide and single metal atoms may be involved.

As stated above, based on *in-situ* XAS observations of the pyrolysis process of various Fe-containing systems, a mechanism based on active Fe atoms obtained from the removal of O from oxides has been proposed. Even though the mechanism targets solid state systems, according to a supplemented experiment by the authors, these active single Fe atoms may be in a gaseous state, without direct contact at elevated temperature, and a small portion of Fe is able to migrate from Fe_2O_3 into N-doped carbon in the form of Fe ADMs. It is not yet clear whether such a mechanism applies to systems containing other metal species, but there have been several studies that found similar phenomena in metals other than Fe. Yang *et al.* reported the thermal emission of Cu atoms from Cu_2O into an N-doped carbon framework to fabricate Cu ADMCs. In their study, MoO_3 and SnO_2 powders were shown to be effective through thermal emission to realize corresponding ADMCs[156].

OUTLOOK AND CHALLENGES

There is no doubt that ADMCs have become the star material in various fields and are gaining more attention from researchers who are trying to widen their application. After years of exploration, several chemical procedures have been proven effective and controllable in fabricating ADMCs. For studies on the formation mechanism, despite the progress made in recent years with the aid of high-end techniques, especially in-temperature XAS and TEM, the composition evolution pathway according to which ADMCs are formed during the thermal reaction is not yet fully and completely understood. Further investigation of the common phenomena is still valuable, for example, the interaction between metal atoms and the surrounding coordination environment and the role pyrolysis parameters play in the evolution of metal moieties. Hopefully, a better understanding would grant us more controllability over the thermal-chemical reactions, thus promoting research on novel fabrication methods, especially those able to precisely manipulate the local structure of ADMs, for example, multi-atom centers with well-defined structures and second and even further coordination shells. Furthermore, methods with high atomic efficiency, low energy consumption, and large-scale production prospects should be developed for possible application at the industrial level.

Notably, despite the progress made in recent years, the formation mechanism of ADMCs is far from being uncovered. There are a few challenges for researchers to pay conscious effort to. The first is to understand the formation of ADMSs to a greater extent. In this review, the formation mechanism is limited to the changes during the transformation from metal precursors to ADMs, without considering the nearby carbon structure. It is discovered that the second or even third coordination shells of the metal center play an important part in the performance of ADMs. Thus, understanding the formation of the entire ADMSs to a greater extent is a valuable yet challenging task. Another challenge we are facing today is to uncover the formation mechanisms of newly-emerged double-atom or even triple-atom ADMs, which are less studied and remain unknown. Uncovering how two or more atoms favorably attract and coordinate on the support is critical for the controllable fabrication of such material.

DECLARATIONS

Authors' contributions

Proposed the topic of this review: Du C
Prepared the manuscript references data: Du J, Yan Y
Prepared the manuscript: Han G, Zhang W, Li L
Collectively discussed and revised the manuscript: Geng L, Tong Y

Availability of data and materials

Not applicable.

Financial support and sponsorship

This work is financially supported by the National Natural Science Foundation of China (Grant No. 51634003) and Heilongjiang Touyan Innovation Team Program (HITTY-20190033).

Conflicts of interest

All authors declared that there are no conflicts of interest.

Ethical approval and consent to participate

Not applicable.

Consent for publication

Not applicable.

Copyright

REFERENCES

1. bp statistical review of world energy 2020. Available from: https://www.bp.com/content/dam/bp/business-sites/en/global/corporate/pdfs/energy-economics/statistical-review/bp-stats-review-2020-full-report.pdf [Last accessed on 27 March 2023].
2. bp statistical review of world energy 2021. Available from: https://www.bp.com/content/dam/bp/business-sites/en/global/corporate/pdfs/energy-economics/statistical-review/bp-stats-review-2021-full-report.pdf [Last accessed on 27 March 2023].
3. Liu Q, Ranocchiari M, van Bokhoven JA. Catalyst overcoating engineering towards high-performance electrocatalysis. *Chem Soc Rev* 2022;51:188-236. DOI PubMed
4. Zhang Z, Liu J, Curcio A, et al. Atomically dispersed materials for rechargeable batteries. *Nano Energy* 2020;76:105085. DOI
5. Venkateswara Raju C, Hwan Cho C, Mohana Rani G, et al. Emerging insights into the use of carbon-based nanomaterials for the electrochemical detection of heavy metal ions. *Coord Chem Rev* 2023;476:214920. DOI
6. Dong F, Wu M, Chen Z, et al. Atomically dispersed transition metal-nitrogen-carbon bifunctional oxygen electrocatalysts for zinc-air batteries: recent advances and future perspectives. *Nanomicro Lett* 2021;14:36. DOI PubMed PMC
7. Li W, Guo Z, Yang J, et al. Advanced strategies for stabilizing single-atom catalysts for energy storage and conversion. *Electrochem Energy Rev* 2022;5:9. DOI
8. Yang X, Priest C, Hou Y, Wu G. Atomically dispersed dual-metal-site PGM-free electrocatalysts for oxygen reduction reaction: opportunities and challenges. *SusMat* 2022;2:569-90. DOI
9. Wang J, Liu W, Luo G, et al. Synergistic effect of well-defined dual sites boosting the oxygen reduction reaction. *Energy Environ Sci* 2018;11:3375-9. DOI
10. He T, Chen Y, Liu Q, et al. Theory-guided regulation of FeN_4 spin state by neighboring Cu atoms for enhanced oxygen reduction electrocatalysis in flexible metal-air batteries. *Angew Chem Int Ed* 2022;61:e202201007. DOI PubMed
11. Xiao M, Zhu J, Li G, et al. A single-atom iridium heterogeneous catalyst in oxygen reduction reaction. *Angew Chem Int Ed* 2019;58:9640-5. DOI PubMed
12. Zhang N, Zhou T, Chen M, et al. High-purity pyrrole-type FeN_4 sites as a superior oxygen reduction electrocatalyst. *Energy Environ Sci* 2020;13:111-8. DOI
13. Liu D, Li X, Chen S, et al. Atomically dispersed platinum supported on curved carbon supports for efficient electrocatalytic hydrogen evolution. *Nat Energy* 2019;4:512-8. DOI
14. Mu X, Gu X, Dai S, et al. Breaking the symmetry of single-atom catalysts enables an extremely low energy barrier and high stability for large-current-density water splitting. *Energy Environ Sci* 2022;15:4048-57. DOI
15. Li BQ, Zhao CX, Liu JN, Zhang Q. Electrosynthesis of hydrogen peroxide synergistically catalyzed by atomic $Co\text{-}N_x\text{-}C$ sites and oxygen functional groups in noble-metal-free electrocatalysts. *Adv Mater* 2019;31:e1808173. DOI
16. Pan F, Li B, Sarnello E, et al. Pore-edge tailoring of single-atom iron-nitrogen sites on graphene for enhanced CO_2 reduction. *ACS Catal* 2020;10:10803-11. DOI
17. Zang W, Yang T, Zou H, et al. Copper single atoms anchored in porous nitrogen-doped carbon as efficient pH-universal catalysts for the nitrogen reduction reaction. *ACS Catal* 2019;9:10166-73. DOI
18. Gokana MR, Wu C, Motora KG, Qi JY, Yen W. Effects of patterned electrode on near infrared light-triggered cesium tungsten bronze/poly(vinylidene)fluoride nanocomposite-based pyroelectric nanogenerator for energy harvesting. *J Power Sources* 2022;536:231524. DOI
19. Chen S, Luo T, Li X, et al. Identification of the highly active $Co\text{-}N_4$ coordination motif for selective oxygen reduction to hydrogen peroxide. *J Am Chem Soc* 2022;144:14505-16. DOI
20. Du Z, Chen X, Hu W, et al. Cobalt in nitrogen-doped graphene as single-atom catalyst for high-sulfur content lithium-sulfur batteries. *J Am Chem Soc* 2019;141:3977-85. DOI PubMed
21. Wang P, Ren Y, Wang R, et al. Atomically dispersed cobalt catalyst anchored on nitrogen-doped carbon nanosheets for lithium-oxygen batteries. *Nat Commun* 2020;11:1576. DOI
22. Xia Q, Zhai Y, Zhao L, et al. Carbon-supported single-atom catalysts for advanced rechargeable metal-air batteries. *Energy Mater* 2022;2:200015. DOI
23. Hu X, Luo G, Zhao Q, et al. Ru single atoms on N-doped carbon by spatial confinement and ionic substitution strategies for high-performance $Li\text{-}O_2$ batteries. *J Am Chem Soc* 2020;142:16776-86. DOI
24. Li X, Han G, Lou S, et al. Tailoring lithium-peroxide reaction kinetics with CuN_2C_2 single-atom moieties for lithium-oxygen batteries. *Nano Energy* 2022;93:106810. DOI
25. Yang T, Qian T, Sun Y, Zhong J, Rosei F, Yan C. Mega high utilization of sodium metal anodes enabled by single zinc atom sites. *Nano Lett* 2019;19:7827-35. DOI PubMed

26. Lu C, Fang R, Chen X. Single-atom catalytic materials for advanced battery systems. *Adv Mater* 2020;32:e1906548. DOI PubMed
27. Yang X, Zheng Y, Yang J, et al. Modeling Fe/N/C catalysts in monolayer graphene. *ACS Catal* 2017;7:139-45. DOI
28. Yang XF, Wang A, Qiao B, Li J, Liu J, Zhang T. Single-atom catalysts: a new frontier in heterogeneous catalysis. *ACC Chem Res* 2013;46:1740-8. DOI PubMed
29. Ji S, Chen Y, Wang X, Zhang Z, Wang D, Li Y. Chemical synthesis of single atomic site catalysts. *Chem Rev* 2020;120:11900-55. DOI PubMed
30. Boucher MB, Zugic B, Cladaras G, et al. Single atom alloy surface analogs in $Pd_{0.18}Cu_{15}$ nanoparticles for selective hydrogenation reactions. *Phys Chem Chem Phys* 2013;15:12187-96. DOI PubMed
31. Lou Y, Liu J. CO oxidation on metal oxide supported single Pt atoms: the role of the support. *Ind Eng Chem Res* 2017;56:6916-25. DOI
32. Zhang J, Liu J, Xi L, et al. Single-atom Au/NiFe layered double hydroxide electrocatalyst: probing the origin of activity for oxygen evolution reaction. *J Am Chem Soc* 2018;140:3876-9. DOI PubMed
33. Zhao D, Chen Z, Yang W, et al. MXene (Ti_3C_2) vacancy-confined single-atom catalyst for efficient functionalization of CO_2. *J Am Chem Soc* 2019;141:4086-93. DOI PubMed
34. Zhang B, Asakura H, Zhang J, Zhang J, De S, Yan N. Stabilizing a platinum1 single-atom catalyst on supported phosphomolybdic acid without compromising hydrogenation activity. *Angew Chem Int Ed* 2016;55:8319-23. DOI PubMed
35. Zhang B, Asakura H, Yan N. Atomically dispersed rhodium on self-assembled phosphotungstic acid: structural features and catalytic CO oxidation properties. *Ind Eng Chem Res* 2017;56:3578-87. DOI
36. Sakamoto R, Toyoda R, Jingyan G, et al. Coordination chemistry for innovative carbon-related materials. *Coord Chem Rev* 2022;466:214577. DOI
37. Umapathi R, Ghoreishian SM, Sonwal S, Rani GM, Huh YS. Portable electrochemical sensing methodologies for on-site detection of pesticide residues in fruits and vegetables. *Coord Chem Rev* 2022;453:214305. DOI
38. Bakandritsos A, Kadam RG, Kumar P, et al. Mixed-valence single-atom catalyst derived from functionalized graphene. *Adv Mater* 2019;31:e1900323. DOI PubMed
39. Liu Z, Li S, Yang J, et al. Ultrafast construction of oxygen-containing scaffold over graphite for trapping Ni^{2+} into single atom catalysts. *ACS Nano* 2020;14:11662-9. DOI PubMed
40. Han G, Zhang X, Liu W, et al. Substrate strain tunes operando geometric distortion and oxygen reduction activity of CuN_2C_2 single-atom sites. *Nat Commun* 2021;12:6335. DOI PubMed PMC
41. Li J, Jiang YF, Wang Q, et al. A general strategy for preparing pyrrolic-N_4 type single-atom catalysts via pre-located isolated atoms. *Nat Commun* 2021;12:6806. DOI PubMed PMC
42. Yan H, Zhao X, Guo N, et al. Atomic engineering of high-density isolated Co atoms on graphene with proximal-atom controlled reaction selectivity. *Nat Commun* 2018;9:3197. DOI PubMed PMC
43. Mehmood A, Pampel J, Ali G, Ha HY, Ruiz-zepeda F, Fellinger T. Facile metal coordination of active site imprinted nitrogen doped carbons for the conservative preparation of non-noble metal oxygen reduction electrocatalysts. *Adv Energy Mater* 2018;8:1701771. DOI
44. Hai X, Zhao X, Guo N, et al. Engineering local and global structures of single Co atoms for a superior oxygen reduction reaction. *ACS Catal* 2020;10:5862-70. DOI
45. Wang X, Chen Z, Zhao X, et al. Regulation of coordination number over single Co sites: triggering the efficient electroreduction of CO_2. *Angew Chem Int Ed* 2018;57:1944-8. DOI PubMed
46. Pan Y, Chen Y, Wu K, et al. Regulating the coordination structure of single-atom Fe-N_xC_y catalytic sites for benzene oxidation. *Nat Commun* 2019;10:4290. DOI PubMed PMC
47. Zhai P, Wang T, Yang W, et al. Uniform lithium deposition assisted by single-atom doping toward high-performance lithium metal anodes. *Adv Energy Mater* 2019;9:1804019. DOI
48. Ha M, Kim DY, Umer M, Gladkikh V, Myung CW, Kim KS. Tuning metal single atoms embedded in N_xC_y moieties toward high-performance electrocatalysis. *Energy Environ Sci* 2021;14:3455-68. DOI
49. Li J, Zhang H, Samarakoon W, et al. Thermally driven structure and performance evolution of atomically dispersed FeN_4 sites for oxygen reduction. *Angew Chem Int Ed* 2019;58:18971-80. DOI PubMed
50. Chen K, Liu K, An P, et al. Iron phthalocyanine with coordination induced electronic localization to boost oxygen reduction reaction. *Nat Commun* 2020;11:4173. DOI PubMed PMC
51. Li Z, Zhuang Z, Lv F, et al. The marriage of the FeN_4 moiety and MXene boosts oxygen reduction catalysis: Fe 3D electron delocalization matters. *Adv Mater* 2018;30:e1803220. DOI PubMed
52. Cui X, Xiao J, Wu Y, et al. A graphene composite material with single cobalt active sites: a highly efficient counter electrode for dye-sensitized solar cells. *Angew Chem Int Ed* 2016;55:6708-12. DOI PubMed
53. Marshall-Roth T, Libretto NJ, Wrobel AT, et al. A pyridinic Fe-N_4 macrocycle models the active sites in Fe/N-doped carbon electrocatalysts. *Nat Commun* 2020;11:5283. DOI
54. Sa YJ, Seo DJ, Woo J, et al. A general approach to preferential formation of active Fe-N_x sites in Fe-N/C electrocatalysts for efficient oxygen reduction reaction. *J Am Chem Soc* 2016;138:15046-56. DOI
55. Wang Q, Ina T, Chen WT, et al. Evolution of Zn(II) single atom catalyst sites during the pyrolysis-induced transformation of ZIF-8 to N-doped carbons. *Sci Bull* 2020;65:1743-51. DOI PubMed

56. Jahnke H, Schönborn M, Zimmermann G. Organic dyestuffs as catalysts for fuel cells. In: Schäfer FP, Gerischer H, Willig F, et al., editors. Physical and chemical applications of dyestuffs. Berlin/Heidelberg: Springer-Verlag; 1976. pp. 133-81. DOI PubMed
57. Gupta S, Tryk D, Bae I, Aldred W, Yeager E. Heat-treated polyacrylonitrile-based catalysts for oxygen electroreduction. *J Appl Electrochem* 1989;19:19-27. DOI
58. Li L, Wen Y, Han G, et al. Tailoring the stability of Fe-N-C via pyridinic nitrogen for acid oxygen reduction reaction. *Chem Eng J* 2022;437:135320. DOI
59. Sun Y, Silvioli L, Sahraie NR, et al. Activity-selectivity trends in the electrochemical production of hydrogen peroxide over single-site metal-nitrogen-carbon catalysts. *J Am Chem Soc* 2019;141:12372-81. DOI PubMed
60. Ding T, Liu X, Tao Z, et al. Atomically precise dinuclear site active toward electrocatalytic CO_2 reduction. *J Am Chem Soc* 2021;143:11317-24. DOI PubMed
61. Hai X, Xi S, Mitchell S, et al. Scalable two-step annealing method for preparing ultra-high-density single-atom catalyst libraries. *Nat Nanotechnol* 2022;17:174-81. DOI
62. Gao J, Yang HB, Huang X, et al. Enabling direct H_2O_2 production in acidic media through rational design of transition metal single atom catalyst. *Chem* 2020;6:658-74. DOI
63. Zhang N, Zhou T, Ge J, et al. High-density planar-like Fe_2N_6 structure catalyzes efficient oxygen reduction. *Matter* 2020;3:509-21. DOI
64. Xiao M, Gao L, Wang Y, et al. Engineering energy level of metal center: Ru single-atom site for efficient and durable oxygen reduction catalysis. *J Am Chem Soc* 2019;141:19800-6. DOI PubMed
65. Li X, Huang X, Xi S, et al. Single cobalt atoms anchored on porous N-doped graphene with dual reaction sites for efficient fenton-like catalysis. *J Am Chem Soc* 2018;140:12469-75. DOI PubMed
66. Jiao L, Wan G, Zhang R, Zhou H, Yu S, Jiang H. From metal-organic frameworks to single-atom Fe implanted N-doped porous carbons: efficient oxygen reduction in both alkaline and acidic media. *Angew Chem Int Ed* 2018;130:8661-5. DOI PubMed
67. Chen W, Pei J, He CT, et al. Single tungsten atoms supported on MOF-derived N-doped carbon for robust electrochemical hydrogen evolution. *Adv Mater* 2018;30:e1800396. DOI PubMed
68. Yang Q, Xu W, Gong S, et al. Atomically dispersed lewis acid sites boost 2-electron oxygen reduction activity of carbon-based catalysts. *Nat Commun* 2020;11:5478. DOI PubMed PMC
69. Al-Zoubi T, Zhou Y, Yin X, et al. Preparation of nonprecious metal electrocatalysts for the reduction of oxygen using a low-temperature sacrificial metal. *J Am Chem Soc* 2020;142:5477-81. DOI PubMed
70. Yang Y, Mao K, Gao S, et al. O-, N-atoms-coordinated Mn cofactors within a graphene framework as bioinspired oxygen reduction reaction electrocatalysts. *Adv Mater* 2018;30:e1801732. DOI PubMed
71. Zhang E, Wang T, Yu K, et al. Bismuth single atoms resulting from transformation of metal-organic frameworks and their use as electrocatalysts for CO_2 reduction. *J Am Chem Soc* 2019;141:16569-73. DOI PubMed
72. Phan A, Doonan CJ, Uribe-Romo FJ, Knobler CB, O'Keeffe M, Yaghi OM. Synthesis, structure, and carbon dioxide capture properties of zeolitic imidazolate frameworks. *ACC Chem Res* 2010;43:58-67. DOI PubMed
73. Chen M, Li X, Yang F, et al. Atomically dispersed MnN_4 catalysts via environmentally benign aqueous synthesis for oxygen reduction: mechanistic understanding of activity and stability improvements. *ACS Catal* 2020;10:10523-34. DOI
74. Li Z, Chen Y, Ji S, et al. Iridium single-atom catalyst on nitrogen-doped carbon for formic acid oxidation synthesized using a general host-guest strategy. *Nat Chem* 2020;12:764-72. DOI PubMed
75. Xie X, He C, Li B, et al. Performance enhancement and degradation mechanism identification of a single-atom Co-N-C catalyst for proton exchange membrane fuel cells. *Nat Catal* 2020;3:1044-54. DOI
76. Wang J, Han G, Wang L, et al. ZIF-8 with ferrocene encapsulated: a promising precursor to single-atom Fe embedded nitrogen-doped carbon as highly efficient catalyst for oxygen electroreduction. *Small* 2018;14:e1704282. DOI PubMed
77. Ji S, Chen Y, Zhao S, et al. Atomically dispersed ruthenium species inside metal-organic frameworks: combining the high activity of atomic sites and the molecular sieving effect of MOFs. *Angew Chem Int Ed* 2019;58:4271-5. DOI PubMed
78. Jiang R, Li L, Sheng T, Hu G, Chen Y, Wang L. Edge-site engineering of atomically dispersed Fe-N_4 by selective C-N bond cleavage for enhanced oxygen reduction reaction activities. *J Am Chem Soc* 2018;140:11594-8. DOI
79. Wan X, Liu X, Li Y, et al. Fe-N-C electrocatalyst with dense active sites and efficient mass transport for high-performance proton exchange membrane fuel cells. *Nat Catal* 2019;2:259-68. DOI
80. Xiong Y, Dong J, Huang ZQ, et al. Single-atom Rh/N-doped carbon electrocatalyst for formic acid oxidation. *Nat Nanotechnol* 2020;15:390-7. DOI PubMed
81. Chen Y, Ji S, Wang Y, et al. Isolated single iron atoms anchored on N-doped porous carbon as an efficient electrocatalyst for the oxygen reduction reaction. *Angew Chem Int Ed* 2017;129:7041-5. DOI PubMed
82. Wang H, Grabstanowicz LR, Barkholtz HM, et al. Impacts of imidazolate ligand on performance of zeolitic-imidazolate framework-derived oxygen reduction catalysts. *ACS Energy Lett* 2019;4:2500-7. DOI
83. Xiao M, Zhu J, Ma L, et al. Microporous framework induced synthesis of single-atom dispersed Fe-N-C acidic ORR catalyst and its in situ reduced Fe-N_4 active site identification revealed by X-ray absorption spectroscopy. *ACS Catal* 2018;8:2824-32. DOI
84. Li J, Chen M, Cullen DA, et al. Atomically dispersed manganese catalysts for oxygen reduction in proton-exchange membrane fuel cells. *Nat Catal* 2018;1:935-45. DOI
85. Zhu M, Zhao C, Liu X, et al. Single atomic cerium sites with a high coordination number for efficient oxygen reduction in proton-

exchange membrane fuel cells. *ACS Catal* 2021;11:3923-9. DOI
86. Liu Q, Li Y, Zheng L, et al. Sequential synthesis and active-site coordination principle of precious metal single-atom catalysts for oxygen reduction reaction and PEM fuel cells. *Adv Energy Mater* 2020;10:2000689. DOI
87. Liu Q, Liu X, Zheng L, Shui J. The solid-phase synthesis of an Fe-N-C electrocatalyst for high-power proton-exchange membrane fuel cells. *Angew Chem Int Ed* 2018;57:1204-8. DOI PubMed
88. Ye W, Chen S, Lin Y, et al. Precisely tuning the number of fe atoms in clusters on N-doped carbon toward acidic oxygen reduction reaction. *Chem* 2019;5:2865-78. DOI
89. Ye Y, Cai F, Li H, et al. Surface functionalization of ZIF-8 with ammonium ferric citrate toward high exposure of Fe-N active sites for efficient oxygen and carbon dioxide electroreduction. *Nano Energy* 2017;38:281-9. DOI
90. Liu M, Li N, Cao S, et al. A “pre-constrained metal twins” strategy to prepare efficient dual-metal-atom catalysts for cooperative oxygen electrocatalysis. *Adv Mater* 2022;34:e2107421. DOI
91. Wan J, Zhao Z, Shang H, et al. In situ phosphatizing of triphenylphosphine encapsulated within metal-organic frameworks to design atomic Co_1-P_1N_3 interfacial structure for promoting catalytic performance. *J Am Chem Soc* 2020;142:8431-9. DOI PubMed
92. Liu J, Kong X, Zheng L, Guo X, Liu X, Shui J. Rare earth single-atom catalysts for nitrogen and carbon dioxide reduction. *ACS Nano* 2020;14:1093-101. DOI PubMed
93. Wang J, Huang Z, Liu W, et al. Design of N-coordinated dual-metal sites: a stable and active Pt-free catalyst for acidic oxygen reduction reaction. *J Am Chem Soc* 2017;139:17281-4. DOI PubMed
94. Xiao M, Chen Y, Zhu J, et al. Climbing the apex of the ORR volcano plot via binuclear site construction: electronic and geometric engineering. *J Am Chem Soc* 2019;141:17763-70. DOI PubMed
95. Ren W, Tan X, Yang W, et al. Isolated diatomic Ni-Fe metal-nitrogen sites for synergistic electroreduction of CO_2. *Angew Chem Int Ed* 2019;58:6972-6. DOI PubMed
96. Wu J, Zhang Q, Wang J, Huang X, Bai H. A self-assembly route to porous polyaniline/reduced graphene oxide composite materials with molecular-level uniformity for high-performance supercapacitors. *Energy Environ Sci* 2018;11:1280-6. DOI
97. An H, Zhang R, Li Z, Zhou L, Shao M, Wei M. Highly efficient metal-free electrocatalysts toward oxygen reduction derived from carbon nanotubes@polypyrrole core-shell hybrids. *J Mater Chem A* 2016;4:18008-14. DOI
98. Li J, Yang Z, Tang D, et al. N-doped carbon nanotubes containing a high concentration of single iron atoms for efficient oxygen reduction. *NPG Asia Mater* 2018;10:e461-e461. DOI
99. Li H, Wen Y, Jiang M, et al. Understanding of neighboring Fe-N_4-C and Co-N_4-C dual active centers for oxygen reduction reaction. *Adv Funct Mater* 2021;31:2011289. DOI
100. Jin Z, Li P, Meng Y, Fang Z, Xiao D, Yu G. Understanding the inter-site distance effect in single-atom catalysts for oxygen electroreduction. *Nat Catal* 2021;4:615-22. DOI
101. Weng CC, Ren JT, Zhao H, Hu ZP, Yuan ZY. Iron-salt thermally emitted strategy to prepare graphene-like carbon nanosheets with trapped Fe species for an efficient electrocatalytic oxygen reduction reaction in the all-pH range. *ACS Appl Mater Interfaces* 2019;11:27823-32. DOI PubMed
102. Zhang M, Wang YG, Chen W, et al. Metal (Hydr)oxides@polymer core-shell strategy to metal single-atom materials. *J Am Chem Soc* 2017;139:10976-9. DOI
103. Han X, Ling X, Yu D, et al. Atomically dispersed binary Co-Ni sites in nitrogen-doped hollow carbon nanocubes for reversible oxygen reduction and evolution. *Adv Mater* 2019;31:e1905622. DOI PubMed
104. Zhou Y, Yu Y, Ma D, et al. Atomic Fe dispersed hierarchical mesoporous Fe-N-C nanostructures for an efficient oxygen reduction reaction. *ACS Catal* 2021;11:74-81. DOI
105. Zhang Z, Zhao X, Xi S, et al. Atomically dispersed cobalt trifunctional electrocatalysts with tailored coordination environment for flexible rechargeable Zn-air battery and self-driven water splitting. *Adv Energy Mater* 2020;10:2002896. DOI
106. Qu Y, Wang L, Li Z, et al. Ambient synthesis of single-atom catalysts from bulk metal via trapping of atoms by surface dangling bonds. *Adv Mater* 2019;31:e1904496. DOI PubMed
107. Zhao Y, Liang J, Wang C, Ma J, Wallace GG. Tunable and efficient tin modified nitrogen-doped carbon nanofibers for electrochemical reduction of aqueous carbon dioxide. *Adv Energy Mater* 2018;8:1702524. DOI
108. Zhang H, Zhou W, Chen T, Guan BY, Li Z, Lou XW. A modular strategy for decorating isolated cobalt atoms into multichannel carbon matrix for electrocatalytic oxygen reduction. *Energy Environ Sci* 2018;11:1980-4. DOI
109. Yang L, Zhang X, Yu L, Hou J, Zhou Z, Lv R. Atomic Fe-N_4/C in flexible carbon fiber membrane as binder-free air cathode for Zn-air batteries with stable cycling over 1,000 h. *Adv Mater* 2022;34:e2105410. DOI
110. Cheng C, Li S, Xia Y, et al. Atomic Fe-N_x coupled open-mesoporous carbon nanofibers for efficient and bioadaptable oxygen electrode in Mg-air batteries. *Adv Mater* 2018:e1802669. DOI
111. Ji D, Fan L, Li L, et al. Atomically transition metals on self-supported porous carbon flake arrays as binder-free air cathode for wearable zinc-air batteries. *Adv Mater* 2019;31:e1808267. DOI PubMed
112. Cheng Q, Yang L, Zou L, et al. Single cobalt atom and N codoped carbon nanofibers as highly durable electrocatalyst for oxygen reduction reaction. *ACS Catal* 2017;7:6864-71. DOI
113. Zhang Z, Sun J, Wang F, Dai L. Efficient oxygen reduction reaction (ORR) catalysts based on single iron atoms dispersed on a hierarchically structured porous carbon framework. *Angew Chem Int Ed* 2018;130:9176-81. DOI PubMed
114. Zhang Z, Gao X, Dou M, Ji J, Wang F. Biomass derived N-doped porous carbon supported single Fe atoms as superior

electrocatalysts for oxygen reduction. *Small* 2017;13:1604290. DOI PubMed
115. Wang C, Chen W, Xia K, Xie N, Wang H, Zhang Y. Silk-derived 2D porous carbon nanosheets with atomically-dispersed Fe-N_x-C sites for highly efficient oxygen reaction catalysts. *Small* 2019;15:e1804966. DOI
116. Yang G, Zhu J, Yuan P, et al. Regulating Fe-spin state by atomically dispersed Mn-N in Fe-N-C catalysts with high oxygen reduction activity. *Nat Commun* 2021;12:1734. DOI PubMed PMC
117. Zeng Z, Gan LY, Bin Yang H, et al. Orbital coupling of hetero-diatomic nickel-iron site for bifunctional electrocatalysis of CO_2 reduction and oxygen evolution. *Nat Commun* 2021;12:4088. DOI PubMed PMC
118. Yang HB, Hung S, Liu S, et al. Atomically dispersed Ni(i) as the active site for electrochemical CO_2 reduction. *Nat Energy* 2018;3:140-7. DOI
119. Zhu C, Fu S, Song J, et al. Self-assembled Fe-N-doped carbon nanotube aerogels with single-atom catalyst feature as high-efficiency oxygen reduction electrocatalysts. *Small* 2017;13:1603407. DOI PubMed
120. Chen Y, Li Z, Zhu Y, et al. Atomic Fe dispersed on N-doped carbon hollow nanospheres for high-efficiency electrocatalytic oxygen reduction. *Adv Mater* 2019;31:e1806312. DOI PubMed
121. Zhang X, Zhang S, Yang Y, et al. A general method for transition metal single atoms anchored on honeycomb-like nitrogen-doped carbon nanosheets. *Adv Mater* 2020;32:e1906905. DOI PubMed
122. Li X, Bi W, Chen M, et al. Exclusive Ni-N_4 sites realize near-unity CO selectivity for electrochemical CO_2 reduction. *J Am Chem Soc* 2017;139:14889-92. DOI PubMed
123. Lu Z, Wang B, Hu Y, et al. An isolated zinc-cobalt atomic pair for highly active and durable oxygen reduction. *Angew Chem Int Ed* 2019;58:2622-6. DOI PubMed
124. Chen W, Pei J, He CT, et al. Rational design of single molybdenum atoms anchored on N-doped carbon for effective hydrogen evolution reaction. *Angew Chem Int Ed* 2017;56:16086-90. DOI PubMed
125. Zhu Y, Cao T, Cao C, et al. One-pot pyrolysis to N-doped graphene with high-density Pt single atomic sites as heterogeneous catalyst for alkene hydrosilylation. *ACS Catal* 2018;8:10004-11. DOI
126. Liu J, Jiao M, Mei B, et al. Carbon-supported divacancy-anchored platinum single-atom electrocatalysts with superhigh Pt utilization for the oxygen reduction reaction. *Angew Chem Int Ed* 2019;58:1163-7. DOI PubMed
127. Kiciński W, Dyjak S. Transition metal impurities in carbon-based materials: Pitfalls, artifacts and deleterious effects. *Carbon* 2020;168:748-845. DOI
128. Tang C, Chen L, Li H, et al. Tailoring acidic oxygen reduction selectivity on single-atom catalysts via modification of first and second coordination spheres. *J Am Chem Soc* 2021;143:7819-27. DOI PubMed
129. Yang H, Shang L, Zhang Q, et al. A universal ligand mediated method for large scale synthesis of transition metal single atom catalysts. *Nat Commun* 2019;10:4585. DOI PubMed PMC
130. Xie X, Liu J, Li T, Song Y, Wang F. Post-formation copper-nitrogen species on carbon black: their chemical structures and active sites for oxygen reduction reaction. *Chem Eur J* 2018;24:9968-75. DOI PubMed
131. Wang Y, Shi R, Shang L, et al. High-efficiency oxygen reduction to hydrogen peroxide catalyzed by nickel single-atom catalysts with tetradentate N_2O_2 coordination in a three-phase flow cell. *Angew Chem Int Ed* 2020;59:13057-62. DOI
132. Gao X, Jang J, Nagase S. Hydrazine and thermal reduction of graphene oxide: reaction mechanisms, product structures, and reaction design. *J Phys Chem C* 2010;114:832-42. DOI
133. Gao C, Chen S, Wang Y, et al. Heterogeneous single-atom catalyst for visible-light-driven high-turnover CO_2 reduction: the role of electron transfer. *Adv Mater* 2018;30:e1704624. DOI PubMed
134. Liang S, Zhu C, Zhang N, et al. A novel single-atom electrocatalyst Ti_1/rGO for efficient cathodic reduction in hybrid photovoltaics. *Adv Mater* 2020;32:e2000478. DOI PubMed
135. Fei H, Dong J, Wan C, et al. Microwave-assisted rapid synthesis of graphene-supported single atomic metals. *Adv Mater* 2018;30:e1802146. DOI PubMed
136. Wan G, Yang C, Zhao W, et al. Anion-regulated selective generation of cobalt sites in carbon: toward superior bifunctional electrocatalysis. *Adv Mater* 2017;29:1703436. DOI PubMed
137. Guo L, Hwang S, Li B, et al. Promoting atomically dispersed mnn_4 sites via sulfur doping for oxygen reduction: unveiling intrinsic activity and degradation in fuel cells. *ACS Nano* 2021;15:6886-99. DOI PubMed
138. Sun W, Du L, Tan Q, et al. Engineering of nitrogen coordinated single cobalt atom moieties for oxygen electroreduction. *ACS Appl Mater Interfaces* 2019;11:41258-66. DOI PubMed
139. Qu Y, Li Z, Chen W, et al. Direct transformation of bulk copper into copper single sites via emitting and trapping of atoms. *Nat Catal* 2018;1:781-6. DOI
140. Qu Y, Chen B, Li Z, et al. Thermal emitting strategy to synthesize atomically dispersed Pt metal sites from bulk Pt metal. *J Am Chem Soc* 2019;141:4505-9. DOI PubMed
141. Jiao L, Li J, Richard LL, et al. Chemical vapour deposition of Fe-N-C oxygen reduction catalysts with full utilization of dense Fe-N_4 sites. *Nat Mater* 2021;20:1385-91. DOI
142. Wu M, Wang K, Yi M, Tong Y, Wang Y, Song S. A facile activation strategy for an MOF-derived metal-free oxygen reduction reaction catalyst: direct access to optimized pore structure and nitrogen species. *ACS Catal* 2017;7:6082-8. DOI
143. Zhang C, Sha J, Fei H, et al. Single-atomic ruthenium catalytic sites on nitrogen-doped graphene for oxygen reduction reaction in acidic medium. *ACS Nano* 2017;11:6930-41. DOI PubMed

144. Bai L, Duan Z, Wen X, Si R, Guan J. Atomically dispersed manganese-based catalysts for efficient catalysis of oxygen reduction reaction. *Appl Catal B Environ* 2019;257:117930. DOI
145. Fei H, Dong J, Arellano-Jiménez MJ, et al. Atomic cobalt on nitrogen-doped graphene for hydrogen generation. *Nat Commun* 2015;6:8668. DOI PubMed PMC
146. Zhang C, Yang S, Wu J, et al. Electrochemical CO_2 reduction with atomic iron-dispersed on nitrogen-doped graphene. *Adv Energy Mater* 2018;8:1703487. DOI
147. Han G, Zheng Y, Zhang X, et al. High loading single-atom Cu dispersed on graphene for efficient oxygen reduction reaction. *Nano Energy* 2019;66:104088. DOI
148. Li Y, Wang S, Wang XS, et al. Facile top-down strategy for direct metal atomization and coordination achieving a high turnover number in CO_2 photoreduction. *J Am Chem Soc* 2020;142:19259-67. DOI PubMed
149. Banhart F. Interactions between metals and carbon nanotubes: at the interface between old and new materials. *Nanoscale* 2009;1:201-13. DOI PubMed
150. Banhart F, Charlier J, Ajayan PM. Dynamic behavior of nickel atoms in graphitic networks. *Phys Rev Lett* 2000;84:686-9. DOI PubMed
151. Liu J, Cao C, Liu X, et al. Direct observation of metal oxide nanoparticles being transformed into metal single atoms with oxygen-coordinated structure and high-loadings. *Angew Chem Int Ed* 2021;60:15248-53. DOI PubMed
152. Wei S, Li A, Liu JC, et al. Direct observation of noble metal nanoparticles transforming to thermally stable single atoms. *Nat Nanotechnol* 2018;13:856-61. DOI PubMed
153. Yang J, Qiu Z, Zhao C, et al. In situ thermal atomization to convert supported nickel nanoparticles into surface-bound nickel single-atom catalysts. *Angew Chem Int Ed* 2018;57:14095-100. DOI PubMed
154. Qiu HJ, Ito Y, Cong W, et al. Nanoporous graphene with single-atom nickel dopants: an efficient and stable catalyst for electrochemical hydrogen production. *Angew Chem Int Ed* 2015;54:14031-5. DOI PubMed
155. Li J, Jiao L, Wegener E, et al. Evolution pathway from iron compounds to $Fe_1(II)$-N_4 sites through gas-phase iron during pyrolysis. *J Am Chem Soc* 2020;142:1417-23. DOI
156. Yang Z, Chen B, Chen W, et al. Directly transforming copper (I) oxide bulk into isolated single-atom copper sites catalyst through gas-transport approach. *Nat Commun* 2019;10:3734. DOI PubMed PMC